DEVELOPMENT OF ACTIVATED CARBON FROM PANDANUS SENDERI STEM FOR THE REMOVAL OF Pb^{2+} AND Ni^{2+} FROM WASTEWATER

BY

ILOKA, Augustine Ugochukwu
MEng/SEET/2016/6392

A THESIS SUBMITTED TO THE POSTGRADUATE SCHOOL
FEDERAL UNIVERSITY OF TECHCNOLOGY, MINNA, NIGERIA
IN PARTIAL FULFILMENT OF THE REQUIREMENTS FOR THE AWARD OF THE
DEGREE OF MASTER OF ENGINEERING IN THE DEPARTMENT OF CHEMICAL
ENGINEERING

NOVEMBER, 2019

ABSTRACT

The released of hazardous and toxic elements like heavy metals from industries into the hydrosphere like oceans, rivers, lakes are a major concern in environment. Natural agents have high adsorption capacities for divalent metal ions. Pandanus is a natural adsorbent and in comparison with others and its availability in Nigeria is cost effective. In this study, the adsorption of heavy metal ions (Pb^{2+} and Ni^{2+}) from sewage wastewater which might occur by environmental contaminant in polluted underground water was investigated in batch condition. Adsorbents was prepared from pandanus senderi stem plant, carbonized at 600 ^{o}C and impregnated with 1M NaOH and 1M H_3PO_4 at 600 ^{o}C in a muffle furnace for 3 hours. The resultant products were analysed using Fourier Transform Infrared and Scanning Electron Microscope Energy Dispersive X-ray, and were also tested to adsorb the heavy metal ions in wastewater at varying pH, dosages, contact time and temperature. The Isotherm, kinetic and thermodynamic studies were carried out on the adsorbents. The Fourier Transform Infrared (FTIR) spectrum identified the present of hydroxyl, carbonyl, carbonxyl and lactone. The Scanning Electron Microscope Energy Dispersive X-ray (SEM/EDX) indicated that phosphoric acid particle activated carbon (H_3PO_4-PAC) has more carbon content of weight concentration (86.38 g) than sodium hydroxide particle activated carbon (NaOH-PAC) (84.42 g) and control activated carbon (CAC) (82.51 g) and the pandanus senderi stem carbon contain minerals like calcium, silver, potassium, silicon, phosphorus, aluminum, magnesium and sodium. The adsorption capacity and metal removal percentage was computed and recorded at various parameters (pH, contact time, dosage and temperature). In this study, the optimum value of pH to Pb^{2+} and Ni^{2+} at 10.197 and 0.4013 mg/g adsorption capacity was 4. The percentage removal for Pb^{2+} increased from 40 to 58% for pH increase from 2.0 to 4.0 while Ni^{2+} increase from 14.4 to 16.1 % for pH increase from 2 to 4. Metal removal for dosage was observed from 0.2 to 0.6 g for Pb^{2+} and decrement was observed in Ni^{2+}. When compared (R^2) values, experimental and predicted value, second order fitted the adsorption. By studying the entropy, enthalpy and mean free energy, Thermodynamic proved the adsorption process are spontaneous and endothermic in nature. It was recommended adsorption column study should be carried out and other chemicals order than NaOH and H_3PO_4 should be used to improve the efficiency. Nevertheless, other heavy metal ions should be used for adsorption studies using pandanus senderi adsorbent.

CHAPTER ONE

1.0 INTRODUCTION

1.1 Background of the Study

The problem of protecting the environment from pollution and contamination by various types of effluent discharges is now in the focus of attention all over the world. The effluent solids consist of spent grains, waste yeast, and total Suspended Dissolves Particles (TSDP). Since most of these TSDP are non-degradable and toxic, their concentration in industrial effluents must be reduced to acceptable levels before discharging them into the environment. Several methods include; coagulation and flocculation, adsorption using various adsorbents, chemical oxidation, anaerobic decolourization and reverse osmosis. Adsorption is preferred over these processes because of its efficiency. The most widely used adsorbent for this purpose is activated carbon, but commercially available activated carbons are expensive and they may not be economical for wastewater treatment. Therefore, non-conventional low cost adsorbents have been also utilized for TSDP removal (Menkiti *et al*., 2014).

Activated Carbons (AC) are made from materials rich in carbon through carbonization and an activation process. A porous structure and its adsorption properties can be obtained in carbonaceous materials via either chemical or physical activation. Zinc Chloride ($ZnCl_2$), KOH, and phosphoric (H_3PO_4) are widely used as chemical activating agents (Shamsuddin *et al*., 2015).

Activated carbon's ability to remove a large variety of compounds from contaminated waters had led to its increased use in the last thirty years. Designing methods for the production of activated carbon in more economic ways is the need of the hour. A range of low cost, easily available,

carbon rich and low ash precursor and sources are thus being explored for the production of activated carbon. (Odubiyi *et al.,* 2012).

Industrial and municipal wastewaters frequently contain heavy metal ions. These heavy metals are considered a serious environmental problem due to their toxicity, long persistence, bio-accumulation and bio-magnifications in food-chain. In fact, heavy metals are toxic to aquatic flora, animals and human beings even at relatively low concentration (Onwu *et al.,* 2014).

Heavy metal are toxic inorganic contaminants that, unlike organic contaminants that can be degraded by microorganisms, must be removed from wastewater before being discharged to the environment. Selection of a treatment process is dependent on the nature of the wastewater and the quality of the effluent desired. The removal of metal ions in industrial effluent using biosorption process has been an area of extensive research because of the presence and accumulation of toxic carcinogenic effect on living species. Some materials investigated for wastewater treatment were cotton, walnut waste, peanut skins, sugar cane wastes and onion skins, coffee grounds, apple waste, wool fibre, bark and other cellulosic materials (Oboh *et al.,* 2009)

Pandanus Senderi originated from Pandanus plant (Screwpine) genus, a tropical plant, known as Pandanus leaves which can be found in the wild, but also widely cultivated area (Mario *et al*., 2019). It functions as an extra flavor in Southeast Asian cooking and the pleasant smell comes from aroma compound of 2acetyl-1-pyrroline. In general, the genus Pandanus is belonging to the family Pandanaceae which comprises about 700 species and widely distributed in tropical and subtropical regions (Fillaeli *et al*., 2019). The leaves have been used as traditional medicine such as antispasmodic, diuretic, and stimulant properties as reported by Shigeyuki *et al*. (2016) for many years. The Pandanus Senderi left some residues after cultivation such as their stems.

Although no much work had done with Pandanus plant on activated carbon only on medicinal areas.

In this research, activated carbon was prepared from locally obtained Nigerian agricultural waste, Pandanus Senderi Stem using H_3PO_4 and NaOH as activating agents. The use of these raw materials in carbon production shows that they are available at low cost, highly available, contain high carbon content, may be effective in the removal of heavy metals and act as a local replacement for existing commercial materials (Sudha *et al.,* 2007).

The report of this work consist of the following; general information about Activated Carbon (AC) and its characteristics that will enable the reader understand the background about AC, an experimental investigation in chemical activation of carbon with Phosphoric acid and Sodium Hydroxide as the chemical reagents and Pandanus stem as the precursor.

1.2   Statement of the Problem

Wastewater is a source of environmental pollutants with adverse effect on human and its environment. The problem of solving contaminated water conventionally has been a big loss to the industries. Many industries are looking and alternative to reduce the cost money spending in conventional treatment. Adsorption with adsorbent is one of options using for the treatment. Currently many industries commonly use different adsorbents for the removal of metal ions. The cost of these adsorbents and problem associated with regeneration of adsorbents had led researchers to find alternate low cost adsorbent. Nowadays, there are numerous commercially available adsorbents which have been used for metal ion removal. Moreover, as the adsorption capacities of various adsorbents are not very large, new modified adsorbents which are more economically available and highly effective are needed for which extensive work is being

conducted. Pandanus is considered as good adsorbent which can be used for the treatment. The added advantage of using Pandanus plant is to obtain a cost effective and efficient adsorbent.

1.3   Aim and Objectives

The aim of this project work is to treat effluent wastewater using activated carbon produced from Pandanus Stem.

The following objectives shall be followed to achieve this aim;

i.   To prepare and characterize activated carbon using Pandanus plant stem via chemical activation process.

ii.   To carry out batch adsorption study by varying (effect of pH, contact time, dosages and temperature).

iii.   Study the adsorption isotherms, kinetics and thermodynamics.

1.4   Justification of the Study

The environment is the most important asset to man and the development of every nation depends largely on its well-managed environment. It is therefore prudent to protect it from pollution. In right of increasing environmental awareness of industrial companies discharging of wastewater in to the water bodies, understanding and controlling the potential environmental liabilities associated with industrial facilities has become increasingly important.

However, sewage wastewater from the WUPA sewage treatment plants may pollute some of water bodies during discharging if the heavy metals are not properly treated and removed, and they make rivers unsafe. It is imperative to remove this heavy metals properly before discharging them into the geo environment. The study is intended to assist by using Pandanus plant stem as

adsorption to remove that heavy metal which has not been used before in WUPA sewage waste water.

1.5   Scope of the Study

In this study, Pandanus senderi stem was used as raw material in preparation of activated carbon. The experiments were carried out in a batch muffle furnace which can be heat up to a temperature of 600 ^{o}C. Sodium hydroxide and phosphoric acid were selected as chemical agents in the impregnation procedure.

Effects of various preparatory conditions including different temperature, contact time, dosages, and pH was studied. The prepared activated carbon was also characterized by using FTIR and SEM to determine the physical characteristics and surface chemistry of the prepared adsorbent. The different adsorbate was used in the adsorption studies which are methylene blue and iodine adsorption number to determine the performances of adsorbent. The experimental data are crucial in determination of the adsorption isotherm of the samples using Langmuir isotherm, Freundlich isotherm model and temkin adsorption isotherm followed by kinetic study. This kinetic study was carried out by using Pseudo-first order, Pseudo-second order and Intra-particle diffusion models. Thermodynamic studies were also done. The validity of each model was confirmed by judging the correlation coefficient R^2

1.6   Significant of Study

One of the used of adsorbent using Pandanus plant is to remove heavy metal ions in sewage wastewater. It is beneficial to our industry because it can improve water quality. When water quality is improved, it is safe for living things especially human being use the water to drinks,

bath, and so on. Other than that, there is a lot application of adsorbent using Pandanus plant, such as in gas purification, gold purification, metal extraction, water purification, medicine, air filters in gas masks and filter masks, filters in compressed air and many other applications. But in this study, it is focus in sewage wastewater, as a sample to remove wastewater pollutant. To choose the most suitable and effective characteristics of adsorbent from Pandanus senderi plant as wastewater pollutant removal, the size of adsorbent has to be prioritized. The size of adsorbent like Powdered Activated Carbon (1.00 – 1.70 mm) was included in this study.

CHAPTER TWO

2.0   LITERATURE REVIEW

2.1   Historical Background of Activated Carbon

The use of activated carbon in the form of carbonized wood began many centuries ago and it has been recognized as one of the most popular and widely used adsorbent in water and wastewater treatment throughout the world. Charcoal, the forerunner of modern activated carbon, is the oldest adsorbent known in water purification. During the 1500s BC, it was used by the Egyptians as a purifying agent and also as an adsorbent for medicinal purposes in which it was used to adsorb odour from rotten wound. The specific adsorptive properties of charcoal were first discovered by Scheele in 1773 for the treatment of gases followed by decolorizing of solutions in 1786 and he provided the first systematic account of the adsorptive power of charcoal in the liquid phase. In the following years, Lowitz established the use of charcoal for the removal of bad taste and odors from water during 1789 to 1790. The credit to develop commercial activated carbon goes to a Swedish Chemist Von Ostreijko who obtained two patents, in 1900 and 1901, on covering the basic concepts of chemical and thermal (or physical) activation of carbon, with metal chlorides and with carbon dioxide and steam, respectively. The process of chemical activation of sawdust with zinc chloride was carried out for the first time in an Austrian plant at Aussing in 1914 on an industrial scale, and also in the dye plant of Bayer in 1915. In this type of activation, pyrolytical heating of the carbonaceous material was performed in the presence of dehydrating chemicals such as, zinc chloride or phosphoric acid. (Amit *et al*., 2013).

Fontanna in 1777 disclosed an experiment in which glowing charcoal was plunged under mercury and allowed to rise into an inverted tube containing a gas, whereupon much of the gas disappeared. In 1794, natural forms of activated carbon, such as charred animal bones (called bone black), were used for the refinement of sugar. Since the 1800's, production of activated carbon moved from woody precursors and bones to various other precursors in search of more effective adsorbents. Since the 1980's, attention has shifted to the production of activated carbon from low cost materials. Sebata *et al*. (2013) prepared activated carbon from Bambara Rroundnut Hulls by impregnation with 0.1 M Nitric acid in a one-step carbonization process. They studied the effect of carbonization temperature on the surface area of the produced carbons and found that the optimum temperature for atrazine adsorption was 25 °C and the amount of atrazine adsorbed decrease with the increase in temperature suggesting the adsorption was exothermic in nature. Kwaghger and Adejoh (2012) prepared activated carbon by carbonizing mange nuts using $ZnCl_2$ as activating agent at carbonization temperature of 500 °C in one hour. They found that percentage yield of activated carbon increased with high surface and low ash content. The produced carbons were tested for adsorption of Cd^{2+} and the most effective activated carbon for the adsorption process was produced at concentration, impregnation ratio and activation time at 65.85 % 1:28 and 4.95 respectively. They also carried out isotherm studies of the adsorption process and found that the adsorption of Cd^{2+} was better described by Langmuir isotherm than Freundlich isotherm. Moreno-Pirajan *et al.* (2012) prepared activated carbon by pyrolysis of Mangifera Indica Seed in the presence of NaOH and KOH and carried out chemical characterizations of the prepared carbons. They found that the pyrolysis of seeds mango impregnated with NaOH and KOH produced materials with a well-developed pore structure and

very high adsorption capacities, making possible to attain surface area of very high as 1987 m^2/g and pore volume was as large at 1.18 cm^3/g.

Akpen *et al*. (2017) prepared carbon from Mango Seed Endocarp by two different impregnation ratio carbonization before activation and after activation with $ZnCl_2$ at 500 ^{o}C for two hours. They studied the effect of the impregnation ratio on the removal of the colour from textile wastewater. Their results show that the CBA is a better adsorbent for the removal of colour from textile wastewater compared to ABC and the highest percentage removal of colour was achieved by CBA was used for determining optimum condition for test carbon for colour removal.

Rajeshwar *et al*. (2011) prepared activated charcoal from Lapsi Seed and the produced carbon was found to have a surface area of 630.80 m^2/g and porosity of 0.5 ml/g. The carbon was tested for adsorption of Pb^{2+} ion from aqueous solution and they found that adsorption increased with increase in pH up to a value of 5, and the continued increase in adsorptive capacities of Pb^{2+} with increase in pH is due to the decrease in H^{+} ion concentration as pH value increases and adsorption equilibrium was attained after 80 minutes.

Okoroigwe *et al*. (2013) prepared activated carbon from Palm Kernel Shells by submerging them with 60 % H_4PO_3 as activating agent and divided into two. The first samples were left for 48 hours and the second samples for 72 hours after which them were carbonized for 600 ^{o}C at 3 hours. They found that ACs produced upon soaking the feedstock in acid for 48 hours and 3 hours carbonization at 600 ^{o}C is better than the one produced at 72 hours soaking time and 3 hours carbonization at 600 ^{o}C separately. They further discovered that duration of carbonization increased the pore volume of the test samples while impregnation period decreased the pore volumes.

Arivoli *et al.* (2009) prepared activated carbon from banana bark by chemical activation using concentrated Sulphuric acid as activating agent and carbonizing in a furnace at 600 $^{\circ}$C for twelve hours. The produced activated carbon was tested for its efficiency in removing chromium ion. The effects of agitation time, initial chromium ion concentration, carbon dose, pH and temperature on the adsorption of the metal ion were studied. Their results show that percent adsorption decreased while the actual amount of chromium ion adsorbed per unit mass of activated carbon increased with increase in initial chromium ion concentration from 10 to 60 mg/L. Both percent adsorption and actual amount of chromium ion adsorbed per unit mass of activated carbon increased with increase in temperature from 30 to 60 $^{\circ}$ C. Percent adsorption also increased with increase in activated carbon dosage from 0.5 to 5 mg/L and with increase in pH up to pH value of 7, beyond which the percent adsorption decreased with further increase in pH. The adsorption followed first order kinetic model and the rate was mainly controlled by intra-particle diffusion. The adsorption capacity obtained from the Langmuir isotherm plots at initial pH of 7.5 were 40.161, 38.462, 35.700 and 37.979 mg/g at 30, 40, 50 and 60 $^{\circ}$C, respectively.

Buah and Kuma (2012) studied the properties of ACs prepared from Coconut Shells. They investigated the influences of steam as activating agent with molar flow rate of 0.027 mol.h/g. Carbonization temperature in the study was 900 °C. They found that the yield of the ACs decreased with respect to activation time from 100 to 41.2 % after 3 hours of activation. They also found that for the studied range of carbonization temperatures, the activated coconut shells possessed higher iodine number in comparison to the unactivated but carbonized coconut shells. Also, the coconut shell activated charcoal produced by activation prior to carbonization had a greater iodine number than the one produced by carbonization prior to activation. The highest

iodine number was obtained from coconut shell produced by activation prior to carbonization at 500 °C.

Bansal *et al.* (2014) prepared activated carbon from wood chips by chemical activation which was carried out in three different methods; Pre-boiled wood chips (BWC), Formaldehyde-treated Wood Chip (FWC) and Sulphric-treated Wood Chip (SWC). They found that the adsorption capacities of the activated carbons for large molecular weight compounds such as Cu^{2+} were 15.53, 15.53 and 16.86 mg/g for BWC, FWC and SWC respectively. They also found that the maximum removal of the Cu^{2+} was observed at an optimum acidic pH of 5.

Raw Bagasse Pith obtain from cane mill was used by Taha *et al.* (2016) to prepare activated carbon. The activated carbon was prepared by chemical and physical activation using H_4PO_3 as activating agent and carbonizing in a muffle furnace at 600 ^{o}C for one hour. The prepared activated carbon was tested for adsorption of Cationic dye. They found that adsorption increased with increase in the concentration of the dye solution. They also found that the adsorption followed first order kinetics and that Langmuir isotherm described the adsorption process better than the Freundlich isotherm.

Soleimani and Kaghazchi (2008), prepared activated carbon from apricot stones by impregnation with phosphoric acid and carbonization in programmable electrical furnace with heating rate of 5 K/min to a final carbonization temperature of 673 K. The activated carbon had BET surface area of 1387 m^2/g, pore volume of 0.954 ml/g, bulk density of 0.452 g/m^3 and percentage ash content of 0.2. They tested the potential of the activated carbon to adsorb gold ions from aqueous solution and found that adsorption increased with decrease in carbon particle size from 12 – 16 to 35 – 50 mesh size and with increase in carbon dose from 1 to 20 kg/m^3. They found the optimum

pH for the gold adsorption to be 10.5 at which 98.15 % of gold ions were adsorbed onto the activated carbon after three hours.

Haiyan *et al*. (2015) prepared activated carbon from Pinewood and Wheat Straw by chemical activation using concentrated KOH as activating agent and carbonizing in a furnace and heated at a rate of $10\,^{o}$C/min from room temperature to $550\,^{o}$C under a humid N_2 flow (0.5 L/min). They studied the effects of particle size, humidity, the KOH/Char ratio, microwave heating time on the physical characteristics of the ACs. They found that the Iodine number of the pinewood increases by approximately 2.9 % with a reduction in particle size I to size II whereas that of wheat straw ACs, it increases by approximately 3 % with a reduction from size II to size III. They recorded that optimum pinewood and wheat straw ACs had Iodine number of 2207 and 1420 mg/g and carbon yields were 73 and 53 % for pinewood and wheat straw ACs respectively. Increasing the microwave heating time led to an increase in the iodine number.

Akpen *et al.* (2011), produced activated carbon from mango seed shell using $ZnCl_2$ as a chemical activation agent. The produced activated carbon had specific surface area of 16.67 m^2/g. They tested its adsorption behavior with methylene waste water. They studied that MB removal was attained within 40 mins by all the carbon and it was chosen as the optimum contact time.

2.2 Methods of Production of Activated Carbon

Activated carbon can be produced from most carbon containing materials. Various natural and synthetic materials have been used as raw materials for the manufacture of activated carbons. Young fossil materials such as wood, peat and wastes of vegetable origin, which include sawdust, nutshells and fruit stones were preferred in early production procedures since the chars from them can be easily activated yielding reasonably high quality activated carbon. However,

presently, there is an increasing use of various kinds of natural coal which are readily available and relatively cheap, though this still ranks second to the use of wood and other plant materials. Various wastes, such as sulphite liquors, waste lignin and wastes from processing of petroleum and lubricating oil industries have also been used as raw materials for the production of activated carbon. Commercially, the most frequently used raw materials are peat, coal, lignite, wood and coconut shells.

In general, the raw materials to make activated carbon must accomplish a sort of requirements like high carbon content, low mineral content, easily activation, low degradation during storage, and, of course, low cost. The phase of application of an activated carbon also determines the type of raw material to be employed in the production of the carbon. For vapour phase applications, carbon from lignin and wood, which are low density materials and have high volatile content are not very suitable because they have large pore volume but low density. However, the quality of the carbon can be improved by densification, reconstitution or compression during carbonization. Carbons from fruit pits, semi-hard coals, coconut shells and other nut shells, which have higher density than wood and possess high volatile contents, are hard and granular with large micropore volumes and are therefore quite suitable for solution as well as vapour phase application (Sadashir *et al*., 2017). The processing technique to be used for the production of activated carbon depends on the nature and type of raw material available as well as the desired physical form of the activated carbon. The production of activated carbon involves two major steps; carbonization and activation. These processes are carried out after the raw material has been prepared and put in a form that will be easy to handle.

2.3   Preparation of Raw Materials

The following processes are carried out on the raw material to put it in a form suitable for carbonization.

(i) Sizing – This involves breaking down of the raw material into lumps or granules of appropriate sizes, which can be handled effectively in subsequent operations.

(ii) Sieving – This is done using wire gauze in the case of materials with fibre or fluffy particles in order to remove these particles and leave the desired material for carbonization. Winnowing could also be carried out alongside the sieving.

(iii) Reconstitution – This involves pulverization of the raw material followed by agglomeration by extrusion or briquetting. It is usually done on low-density materials in order to improve their quality.

2.3.1   Carbonization

Carbonization is the thermal separation of carbonaceous materials, elimination of organic materials and production of porous fixed carbon. This process is usually carried out in a muffle furnace or in rotary kilns at elevated temperatures. It involves thermal decomposition of the raw material as it is heated under a time schedule to remove the volatile or non-carbon entities leaving basically carbon possessing a partially developed pore structure. Usually, basic microstructure of carbon is formed at 500 ^{o}C, although there may be blockages of the micropores by pyrolytic products, which can only volatilize at higher temperatures. According to Mohamed *et al.* (2017), temperatures below 600 ^{o}C are suitable for the production of chars that are to be activated with steam but this is not an invariable rule. Carbonization product is non-active material as a result of its small surface area.

2.3.2   Activation

This is the process of transforming inert carbon into highly adsorbent material by conferring on it a porous material structure and large specific surface area. The objective is to enhance the volume and enlarge the pores which were created during the carbonization process, and also to create new pores. Activation is of two main types, namely physical and chemical activation.

2.3.2.1 Thermal activation (or physical activation)

It consists of two steps. The first step is thermal carbonization of the raw material, where devolatilization takes place, and it carried out at medium or high temperatures, to produce some char rich in carbon while the second step is activation, where the remaining char is partially gasified with an oxidizing agent (mostly steam) in direct fired furnaces. If both steps are carried out simultaneously, the process is called direct activation (Menendez-Diaz *et al*., 2006).

Physical activation involves the treatment of carbonized materials with oxidizing gases at elevated temperatures between 700 - 1100 ^{o}C. Common gases used include CO_2, steam, and O_2 or a mixture of them to increase the porosity and surface area (Luka *et al*., 2018). This creates more sites for adsorption with the liberation of gases such as H_2, CO_2 and CO. The active oxygen in the activating agent basically burns away the more reactive portions of the carbon skeleton as CO and CO_2. The extent of this depends on the nature of the gas employed and the temperature of activation. The endothermic gasification reactions of carbon with steam and CO_2 with their respective heats of reaction (ΔHr) are shown in equations (2.1) and (2.2).

$$C_{(s)} + H_2O_{(g)} \rightarrow CO_{(g)} + H_{2\,(g)} + 117 \text{ kJ.g}^{-1}\text{.mol}^{-1} \tag{2.1}$$

$$C_{(s)} + CO_{2\,(g)} \rightarrow 2CO_{(g)} + 159 \text{ kJ.g}^{-1}\text{.mol}^{-1} \tag{2.2}$$

The reaction of steam with carbon also produces a side reaction whereby the carbon surface catalyzes an exothermic reaction of CO and steam to yield CO_2 and H_2 as shown in equation (2.3).

$$CO_{(g)} + H_2O_{(g)} \rightarrow CO_{2\,(g)} + H_{2\,(g)} + 42 \text{ kJ.g}^{-1}.\text{mol}^{-1} \qquad (2.3)$$
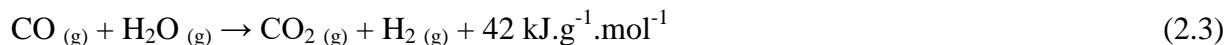
This reaction retards activation, since the $H_{2\,(g)}$ becomes strongly adsorbed at active sites on the carbon surface. In general, steam is preferred to CO_2 as an activation gas because the water molecule has a smaller van der Waals' radius than CO_2 (~3.8Å vs. ~4.8Å). This leads to a faster diffusion of steam in the porous matrix of the carbon and a subsequent faster reaction rate. The reaction of solid carbon and CO_2 (equation 2.2) can be retarded by the addition of $CO_{(g)}$ to drive the thermodynamic equilibrium to the left, which may improve microporous structure through a decreased gasification rate. The process of steam activation produces a carbonaceous substance with many small pores and thus a very large internal surface area. This carbon is then crushed, if desired, to yield a pulverized product.

2.3.2.2 Chemical activation

Chemical activation is typically employed when wood products are used as raw material and it involves impregnation of the feedstock with chemicals either before or after pyrolysis (carbonization). Typical chemicals used as activating agents in chemical activation include phosphoric acid (H_3PO_4), ammonium chloride (NH_4Cl), sulfuric acid (H_2SO_4), potassium sulfide (K_2S), carbonates of alkali metals, and metal chlorides. The common property of chemical activation compounds is to dehydrate the carbonaceous material which usually enhances pyrolytic decomposition and inhibits formation of tar. This process has an advantage over physical activation processes since it normally occurs at temperatures lower than those used in

the latter. This may also benefit the development of a microporous structure. The mechanism of chemical activation is not fully understood. According to Zubrik *et al*. (2017), during chemical activation, the chemistry of pyrolysis is changed and a different, macromolecular network is established with enhanced porosity. However, the chemical detail of this remains unexplored. Distribution of pore sizes in the product depends on the degree of impregnation. Therefore, it is of productive and economic interest to use the ratio of activating agent to raw material that gives the best results. The obtained carbon is then washed to neutral pH and then dried and preserved.

2.4   Characteristics of Activated Carbon

Activated carbon represents substances with high carbon content which have undergone the process of activation. It also refers to carbons in which the adsorptive powers have been supposedly increased by man-made operations. According to Mario *et al.* (2018), activated carbon is a well-known adsorbent due to its extended surface area, high adsorption capacity, fast kinetics and relatively easy regenerations. A generalized definition is that activated carbons also called activated charcoal, is a form of carbon that has been processed with oxygen to create millions of tiny pores between the carbon atoms (Rangari *et al*., 2017). Hence, they are able to adsorb a wide variety of substances and are good adsorbents. Structurally, activated carbon is an amorphous form of carbon. This implies that it has no regular atomic structure unlike the other allotropes (forms) of elemental carbon (diamond, fullerenes or nanotubes). Activated carbon is hydrophobic and non-polar.

2.5   Classifications of Activated Carbon

Activated carbons are complex products which are difficult to classify on the basis of their behavior, surface characteristics and preparation methods. However, some broad classification is made for general purpose based on their physical characteristics.

2.5.1 Powdered activated carbon (PAC)

PAC material is defined as fine activated carbon material. PAC is made up of crushed or ground carbon particles. They are so finely powdered that most of them can easily pass through a designated mesh size. Due to their small size they form large internal surface having small diffusion distance (barrier to adsorption) and large pore diameters. Hence, their rate of adsorption is high and mass transfer problems are very low. PAC is not commonly used in a dedicated vessel, owing to the high head loss that would occur. PAC is generally added directly to other process units, such as raw water intakes, rapid mix basins, clarifiers, and gravity filters. In general, PAC is used to adsorb materials from liquids.

2.5.2 Granulated activated carbon (GAC)

GAC is usually prepared from coal, petroleum, heavy oils, rubber, and the pyrolysis of waste rubber tyres. They come in both granular and extruded form. Granulated activated carbon forms are of larger particle size than the powdered activated carbon forms. Granulated carbons are mainly used for treating water. Their main function includes deodorization and separation of components of flow system. They are generally used for the removal of hazardous and/or pollutant chemicals from wastewater and for purification of water, air and other materials (Menendez-Diaz *et al*., 2006). Hard granules and relatively dust free pellets are usually used for adsorbing gaseous materials in packed beds.

2.5.3 Pelleted activated carbon

They are granulated in smaller size and come in extruded and cylindrical shape with diameters from 0.8 to 5 mm. These are mainly used for gas phase applications because of their low pressure drop, high mechanical strength and low dust content.

2.5.4 Spherical activated carbon

These are usually small and spherical and have high mechanical strength and excellent SO_2 and NO_2 adsorption capacity.

2.5.5 Impregnated carbon

These are porous carbons which have been impregnated with other substances. They are usually prepared for specific applications in air pollution control especially in museums and galleries. Silver loaded activated carbon is used as an adsorbent for purification of domestic water. Drinking water can be obtained from natural water by treating the natural water with a mixture of activated carbon and flocculating agent [$Al(OH)_3$]. Impregnated carbons are also used for the adsorption of H_2S and mercaptans.

2.5.6 Polymers coated carbon

These are porous carbons produced by coating with a biocompatible polymer to give a smooth and permeable coat without blocking the pores. The resulting carbon is useful for hemo-perfusion which is a treatment technique in which large volumes of the patient's blood are passed over an adsorbent substance in order to remove toxic substances from the blood.

2.6   Properties of Activated Carbon

Activated carbon is not a pure carbon. It contains other elements in various proportions depending on the source material and on the mechanism of its production. Such other elements, which are chemically combined with the carbon atoms, include hydrogen, oxygen, nitrogen, sulphur, etc. The adsorptive and catalytic powers of the activated carbons are traced to the presence of these elements in the carbon. The morphology of an activated carbon as observed by an electron microscopy is greatly determined by the raw material that was used for its production. This is as a result of the fact that the nature of the starting material is directly reflected in the final product. The properties of commercially available activated pores available only to small molecule adsorption carbon large and small pores available to both small and large molecule adsorption carbons are responsible for their use as either gas-phase or liquid-phase adsorbents. These properties are grouped into two broad classes; physical and chemical properties.

2.6.1   Physical properties forms

Activated carbons are available in different forms such as symmetrical pellets, irregularly shaped granules, powder and specialties like pre-formed shapes, example, wool and slurry for coating supports. The major forms of activated carbon are the powdered form, the granular form and the pellets. These forms of activated carbon have been described in section 2.3.1.

2.6.1.1 Particle size

This property is important due to the fact that adsorption rate varies inversely with particle size. Mathematically,

$$r\alpha \frac{1}{s} \tag{2.4}$$

where r is the rate of adsorption and s is the particle size. This means that, an increase in particle size will lead to a decrease in adsorption rate while a decrease in particle size will favour high adsorption rate. The finer the particles size of an activated carbon, the better the access to the surface area and the faster the rate of adsorption kinetics. In vapour phase systems, this needs to be considered against pressure drop which will affect energy cost. Careful consideration of particle size distribution can provide significant operating benefits.

2.6.1.2 Abrasion resistance

Abrasion resistance refers to a carbon's ability to withstand degradation during handling and is expressed in terms of abrasion number or handling number. It is an important indicator of an activated carbon's ability to maintain its physical integrity and withstand frictional forces imposed by backwashing and other factors. During handling and use, the harder the activated carbon, the less it will crumble into fine particles which can escape from the system leading to losses. It is estimated by comparing the screen analysis of a carbon before and after subjection to abrasion and shows the mechanical strength of the activated carbon. There are large differences in the hardness of activated carbons, depending on the raw material and activating level. For adsorption of liquids or solids dissolved in liquid, the activated carbon needs mechanical strength enough to support the adhering solutes as they are being adsorbed. For adsorption of gases under high pressure, activated carbon of high mechanical strength is also required due to the fact that high force is associated with increased pressure for a given surface area since pressure is directly proportional to force.

This can be expressed mathematically as equation (2.5) or (2.6).

$$pressure = \frac{forece}{\left(unit\,area\right)} \tag{2.5}$$

$$force = \frac{pressure}{(unit\,area)} \qquad\qquad (2.6)$$

This means that for a constant unit area (surface area of the adsorbent), a rise in the pressure of the adsorbate results in a corresponding rise in the force exerted by the adsorbate on the activated carbon.

2.6.1.3 Bulk density

Apparent or bulk density is a measure of the weight of material that can be contained in a given volume under specified conditions. It is determined by measuring the volume of a weighed sample of activated carbon after tapping till no further reduction in volume occurs. The volume used in this determination includes, in addition to the volume of the skeletal solid, the volume of the voids among the particles and the volume of the pores within the particles. Bulk density of carbon determines how much of it can be contained in a given container. Bulk density is affected by the raw material used and the degree of activation. The density does not affect the effectiveness of the activated carbon measured in adsorption per unit weight, but will have an effect on adsorption per unit volume. Higher density provides greater volume activity.

2.6.1.4 Surface area

Activated carbons have very large surface area, typically ranging from 500 – 1400 m^2g^{-1}. This is an important property of activated carbon as it greatly affects the adsorptive properties of the carbon. Increase in surface area enhances the adsorptive capabilities of activated carbon by exposing a wide surface for physical as well as chemical adsorptions.

2.6.1.5 Pore structure

The amount and distribution of pores in an adsorbent play key role in determining how well adsorbates are adsorbed. Practically, the type of raw material and the method of activation are important parameters which may influence the type of porosity. The pore structure of an activated carbon limits the size of the molecules that can be adsorbed on it. Individual pores can vary greatly in size and shape for different adsorbents and even within the same adsorbent. Pores are usually characterized in terms of their width, meaning the diameter of a cylindrical pore or the distance between two sides of a slit-shaped pore. The pore classification adopted by the International Union of Pure and Applied Chemistry (Sadashiv *et al.,* 2017) is shown in Table 2.1.

Table 2.1: Pore Classifications by Pore Width

Pore Classification	Pore Width
Micropores	Less than 2nm
Mesopores	Between 2 and 50nm
Macropores	More than 50nm

(Sadashiv *et al.,* 2017).

The basis for the pore classifications presented in Table 2.1 is that each size range corresponds to different adsorption effects, as observed in an adsorption isotherm. Physical adsorption of molecules from gas or liquid onto activated carbon takes place in the pores and usually involves 3 steps:

(1) Macro transport: The movement of adsorbate material through the macropore system of the activated carbon

(2) Micro transport: The movement of adsorbate material through the mesopore and micropore system of the activated carbon.

(3) Sorption: The physical attachment of adsorbate material in the mesopores and micropores on the surface of activated carbon.

Pore size is a determinant of efficient adsorption. Within the pores exists an adsorption energy potential which emanates from each pore wall. In the case of physical adsorption, these forces closely resemble dispersion (or van der Waals forces). If large enough, this energy of adsorption is able to capture adsorbate molecules as they enter the pore, adhering the molecules to the pore wall. If the proximity of the pore walls causes overlap of the adsorption fields, as in the case of micropores, the result is an increase in the potential for adsorption. So, although some activated carbons may have lower surface areas and total pore volumes, their smaller pore sizes increase their potential for adsorption. This makes small pores prime candidates for removal of low adsorbate concentrations, where the driving force for diffusional transport of the molecule to the surface is minimal.

The presence of micropores increase the adsorption potentials of carbons over those of nonporous and mesoporous materials. These micropores are responsible for the large surface area of activated carbon particles created during the activation process. It is in the micropores that adsorption largely takes place. The interaction potential in micropores is much greater than that in larger pores due to the closeness of the pore walls, resulting in an enhanced adsorption potential. An adsorbate molecule within a micropore is held there by adsorption forces originating from approximately the ten nearest surface atoms. The forces on adsorbate molecules depend on the distance between adsorbate and adsorbent atoms (pore size) (Sadashiv *et al.*, 2017). The macropores and large mesopores play an extensive role in the molecular transport

process by providing a passage-way to the internal part of the activated carbon into the micropores. They do not contribute substantially to the particle surface area unlike the micropores. Capillary condensation takes place within mesopores, resulting in a hysteresis loop in the adsorption isotherm. In macropores, the pores are so wide that it is almost impossible to map out the isotherm in detail, especially for gaseous adsorbate in which case pressures of the adsorbate would become so close to unity. The more widely the pore sizes are distributed, the more enhanced the adsorptive capacity of the carbon.

2.6.2   Chemical properties

2.6.2.1 pH

The pH of an activated carbon is a measure of the surface acidity/basicity of the carbon. This is the pH of a suspension of the activated carbon in distilled water. The numerical values of the pH are affected by the experimental conditions when carrying out the experiment. A carbon pH of 6 to 8 is acceptable for most application such as sugar decolorization, water treatment, etc. The pH of many of the commercial carbons is due to inorganic components originating from the raw material used or added during the manufacturing process. After activation (with acid) and carbonization, activated carbons are usually washed to bring them to neutral pH.

2.6.2.2 Moisture content

This is determined by drying an isolated portion of an activated carbon in an oven at 105 – 110 ^{o}C until constant weight is attained. This property is important in adsorptive capacity test.

2.6.2.3 Inorganic constituents

Activated carbons contain different inorganic substances, which originate from the raw materials used and also from the ingredients added during the processing of the carbon. However, the total amount of these inorganic constituents varies from one grade of activated carbon to another. The inorganic constituents include:

1. **Ash**

This is the form in which the inorganic constituents of carbon exist after the carbon has undergone complete combustion at controlled temperature. Ash in an activated carbon is an impurity and is not desired. It reduces the overall activity of the activated carbon and reduces the efficiency of re-activation. The metals (Fe_2O_3) can leach out of activated carbon resulting in discoloration. Acid/water soluble ash content is more significant than total ash content. In some carbons, not all inorganic constituents remain as ash after combustion of the carbons. Therefore, in such carbons, the amount of inorganic substances that can be eluted from them is less than the water soluble inorganic substances found in their ash. This is illustrated in Table 2.2.

Table 2.2: Amount of Water Soluble Inorganic Substances in Carbon

Carbon Grade	Found in ash from 100g carbon (g)	Eluted from 100g original carbon (g)
EE	0.75	0.50
FF	0.80	0.41
GG	1.52	1.55

| MM | 2.50 | 1.20 |
| NN | 3.50 | 2.05 |

(Sadashiv *et al.*, 2017)

2.6.2.4 Inorganic constituents as ion exchangers

Some types of activated carbon usually contain a normally soluble inorganic compound bonded to the carbon in the form of an ion exchanger, usually an anion exchanger. These ion exchangers attract free ions in solution or suspension. The capability of an activated carbon to exchange a particular type of ion often depends on the way the carbon is treated.

2.7   Adsorption Phenomena

According to Odubiyi *et al.* (2012) it is a natural process by which molecules of a dissolved compound collection and adhere to the surface of an adsorbent solid. It can also be a physico-chemical process that generally occurs at the interface of fluid-solid phases and is sometimes used to remove certain species that cannot effectively be removed from the wastewater stream by other conventional technologies (Oboh *et al.,* 2009). This becomes feasible only when the substance to be adsorbed is in contact with the adsorbing surface. The adsorbing surface is called the adsorbent while the adsorbed substance is called the adsorbate. The chemical equilibrium which represents the adsorption of molecules on a surface is as follows:

$$A + B \; \rightleftarrows \; AB \tag{2.7}$$

where, A is the adsorbate, B is the adsorbent and AB is the product of the adsorption process. For adsorption of compounds on activated carbon, which is a reversible reaction, molecules continue to accumulate on the surface of the carbon until the rate of the forward reaction

(adsorption process) is equal to the rate of the backward reaction (desorption process). At this point, equilibrium state is attained and no further accumulation of the adsorbate on the adsorbent surface occurs. Hence, adsorption stops. This equilibrium state enables relationship known as adsorption isotherm. Based on the energy associated with adsorption and the type of bond responsible for the adherence of the adsorbate on the adsorbent, adsorption process can be classified into physical and chemical adsorption.

2.7.1 Physical adsorption (physisorption)

This is a weak form of interaction between an adsorbent and adsorbate molecules. The forces involved are similar to van der Waal's forces and the heat evolved during the exothermic adsorption reaction is low (usually of the same magnitude as the enthalpy of condensation < 42 $KJ.mol^{-1}$). This amount of energy can be adsorbed as vibrations of the lattice and dissipated as thermal motion. Because of the energy requirements for the process, equilibrium between the solid surface and the gas molecules is usually easily attained and is readily reversible. The amount of physisorption decreases rapidly as temperature is raised and is generally very small above the critical temperature of the adsorbed specie. Due to the weak force involved in physisorption, the activation energy is low, not more than 42 kJ/mol. The rate of physisorption is very high but the process is non-specific.

Generally, the process of physical adsorption begins as an adsorbate molecule is transported from the bulk adsorbate phase to the surface of the adsorbent. Next, the molecule then diffuses into the pore and then physically bonds with the surface. Heat is usually evolved, making adsorption an exothermic process. In the first step, the bulk adsorbate stream must be intimately mixed with the adsorbent to promote good contact between the two components. In the second

and third stages, the concentration gradient between the amount of adsorbate present in the bulk adsorbate stream and that within the micropore provides the driving force for adsorption.

2.7.2   Chemical adsorption (chemisorption)

This type of adsorption is one in which chemical bond is formed between the adsorbate and the adsorbent. The chemical bond involved is usually covalent bond and the adsorbent tends to find sites that will maximize its co-ordination number with the substrate. Chemisorption is specific and involves forces which are stronger than those associated with physisorption. Hence, the heat of adsorption in this case is high and is of the same order as heat of reaction. This process requires generally high temperature and is often irreversible. Unlike physisorption, in which multilayer coverage is possible, chemisorption does not exceed monolayer coverage. This is because the valence force holding the molecules on the adsorbent surface diminishes rapidly with distance. Generally, chemical adsorption is linked to the porosity and surface chemistry of the carbon, since chemisorption is associated with the number of active sites and carbon surface.

Chemisorption is of two kinds; activated and non-activated chemisorption. In activated chemisorption, high activation energy is involved and the rate varies with temperature according to the finite activation energy (between 8.4 – 83.7 kJ/mol) in the Arrhenius equation (equation 2.8).

$$k = Ae^{\frac{-E}{RT}}$$ (2.8)

where k is the rate of reaction, A is a proportionality constant, E is the activation energy, R is the universal gas constant and T is the absolute temperature. In non-activated chemisorption, the process occurs very rapidly, hence, the activation energy is low, usually close to zero.

2.8   Adsorption Isotherm

Adsorption isotherms are used to understand how the adsorbate molecules are partitioned between the aqueous and solid phases under equilibrium condition. (Norouzi *et al*., 2018). Equilibrium data, commonly known as adsorption isotherms are basic requirements for the design of adsorption system (Suleiman *et al.,* 2013).

The relationship between the concentration of chemical adsorbed (S) and the concentration remaining in the solution (C) at equilibrium is referred as the adsorption isotherm because the experiments are performed at constant temperature. It will describe the equilibrium distribution of solute between the solid and liquid (Mohammad *et al*., 2009)

Surface adsorption is the simplest model of adsorption on a surface by which localized adsorption takes places on an energetically uniform surface without any interaction between adsorbed molecules. The maximum adsorption occurs when the surface is covered by a monolayer of adsorbate (Okafo *et al.,* 2014).

The models used to describe the isotherm function of adsorption include the Langmuir isotherm, Freundlich isotherm, and Temkin isotherm. (Onwu *et al.,* 2014)

2.8.1   Langmuir isotherm model

The basic assumption of Langmuir adsorption isotherm is based on (Taha *et al.,* 2016):

1. The Langmuir isotherm has a theoretical justification.
2. Monolayer coverage of the adsorbate on the surface of adsorbent.
3. Adsorption is a reversible process.
4. The adsorbed molecules do not move on the surface of the adsorbent.

5. They can be lost back to the solution and the enthalpy of adsorption is the same for all molecules independently of how many have been adsorbed.

6. The Langmuir isotherm typically represents well data for single components

Langmuir suggested that adsorption takes place as follows:

$$A + S \underset{K_d}{\overset{K_a}{\rightleftarrows}} AS \tag{2.9}$$

where, A is an adsorbate molecule, S is an adsorption site, k_a corresponds to the rate constant for the adsorption process and k_d corresponds to the rate constant for the desorption process.

At equilibrium, the rate of adsorption is equal to the rate of desorption. On a uniform catalyst surface, the equilibrium condition for a gaseous adsorbate is represented by the following

equation:

$$KaP(1-\theta) = Kd\theta \tag{2.10}$$

where, P is the pressure of the adsorbate, A, and θ is the fractional surface coverage. The required relationship for Langmuir isotherm becomes:

$$\theta = \frac{KP}{1+KP} \tag{2.11}$$

where,

$$K = \frac{K_a}{K_d} = K_o e^{\frac{q}{RT}} \tag{2.12}$$

k_o is a constant and q is the heat of adsorption.

The applicability of the Langmuir isotherm to any gas adsorption process can be tested by the use of equation (2.13), which is a rearranged form of equation (2.11).

$$\frac{P}{\theta} = \frac{1}{K} + P \qquad (2.13)$$

Thus, a plot of (P/θ) against P should yield a straight line graph whose slope is 1 and the intercept is $1/K$. Also, K, which is the adsorption equilibrium constant, should increase with temperature.

For liquid adsorbates, however, the Langmuir isotherm is usually expressed as follows:

$$Q_e = \frac{q_{max}C_e}{K_L + C_e} \qquad (2.14)$$

where, Q_e is the equilibrium value of adsorbate adsorbed per unit weight of adsorbent (mg/g), q_{max} is the maximum amount of metal ions per unit mass of the adsorbent to form a complete monolayer on the surface bound at high C_e (mg/g), C_e is the residual equilibrium concentration of the adsorbate, k_L is the Langmuir's constant and is related to the measure of affinity of the adsorbate for the adsorbent (l/mg) (Onwu *et al.* 2014). For correlation purposes, the equation is rearranged as follows:

$$\frac{C_e}{q_e} = \frac{1}{K_L q_{max}} + \frac{1}{q_{max}} C_e \qquad (2.15)$$

A linearized plot of C_e/q_e against C_e yields a straight line graph which has an intercept and slope which correspond to ($1/K_L.q_{max}$) and ($1/q_{max}$), respectively, from which the q_{max} and K_L can be calculated.

To confirm the favourability of an adsorption process to Langmuir isotherm, the essential features of the isotherm can be expressed in terms of a dimensionless constant known as the separation factor or equation parameter, R_L, which can be calculated by the following equation.

$$R_L = \frac{1}{1 + K_L C_O} \tag{2.16}$$

where, C_o is the initial adsorbate concentration and K_L is the Langmuir constant. The value of R_L explains the nature of the adsorption isotherm to be either favourable if $0 < R_L < 1$, unfavourable if $R_L > 1$, linear if $R_L = 1$ or reversible if $R_L = 0$ (Muhammad *et al.*, 2012).

2.8.2 Freundlich isotherm model

The Freundlich equation assumes that different sites with several adsorption energies are involved in the process of adsorption (Sebata *et al.,* 2013). It therefore incorporates surface heterogeneity of active sites. The Freundlich isotherm can be derived by applying the Langmuir model and assuming that the heat of adsorption, ΔH, is exponentially dependent on the fractional surface coverage, θ (Gupta, 2015). This is expressed in the following equation.

$$\theta = \left(a_o P\right)^{\frac{-RT}{\Delta Hm}} = \left(a_O P\right)^{\frac{RT}{q_m}} = \frac{g}{g_m} \tag{2.17}$$

where,

$$q_m = -\Delta Hm \tag{2.18}$$

$$a_o = \frac{k_a}{k_d} \tag{2.19}$$

P is the pressure of the adsorbate, R is the universal constant, T is the temperature, g is the amount of adsorbate adsorbed by adsorbent, g_m is the amount of adsorbate adsorbed when the surface of the adsorbent is completely covered with a monolayer, k_a is the rate of adsorption and k_d is the rate of desorption.

For purposes of data analysis, the isotherm can be arranged as follows:

$$In[g] = [In(g_m) + (RT/q_m)In(a_o)] + (RT/q_m)In(P)$$

(2.20)

The terms in the brackets are constants at constant temperature. A plot of ln g against ln P yields a straight line whose slope is (RT/q_m), from which q_m can be calculated.

For liquid adsorbates, the Freundlich relationship is shown as follows:

$$q_e = K_F C_e^{1/n}$$

(2.21)

where, 1/n is a heterogeneity factor, which is a measure of intensity of sorption or affinity of the adsorbate for the adsorbent (Taha *et al.,* 2014); K_F is the Freundlich constant.

According Ghasemi *et al* (2014), the Freundlich equation can be linearized as shown in equation (2.22).

$$\log[q_e] = \log[K_F] + \left[\frac{1}{n}\right]\log(C_e)$$

(2.22)

K_F is adsorption capacity and n is the adsorption intensity. The values of n could give an indication on the favorability of sorption. Where n<1, 1<n<2 and 2<n<10 represent poor, moderately difficult and favorable adsorption conditions, respectively.

The constants, K_F and n, are determined by plotting log Ce on the abscissa and log q_e on the ordinate. A best fit of the experimental data provides values for K_F and n based on the y intercept and the slope, respectively. The Freundlich equation is useful in cases where the actual identity of the adsorbate is not known.

2.8.3   Temkin isotherm

The Temkin isotherm assumes that the fall in the heat of sorption is linear rather than logarithmic, as implied in the Freundlich equation. The isotherm can be derived based on assumption that the free energy of adsorption is simply a function of surface coverage. It is a useful tool to estimate the heat of adsorption. The appropriate Langmuir isotherm is as shown in the following equation.

$$\theta/(1-\theta) = (k_a/k_d)P.\exp\left(-H/RT\right) \tag{2.23}$$

This gives the Temkin isotherm to be as shown in equation (1.24) for gaseous adsorbates.

$$In\theta(1-\theta) = InP + \left(\Delta H_o \alpha\theta/RT\right) + InA_O \tag{2.24}$$

where,

$$A_o = a_o \exp\left(q/RT\right) \tag{2.25}$$

α is a positive constant.

If the variation of ln θ/(1 - θ) is taken to be negligible, then equation (2.24) becomes:

$$InP + \left(\Delta H_o \alpha\theta/RT\right) + InA_o = 0 \tag{2.26}$$

This can be rearranged in the form of equation (2.27).

$$\theta = \left(RT \middle/ q_o \alpha \right) In(A_o P) = g \middle/ g_m \tag{2.27}$$

where,

$$q_o = -\Delta H_o \tag{2.28}$$

ΔH_o is the heat of adsorption at zero coverage.

For correlation purposes, the isotherm is expressed as follows:

$$g = \left(g_m RT \middle/ q_o \alpha \right) \left[In(a_o) + \left(g_m \frac{q_o}{RT} \right) \right] + \left(g_m RT \middle/ q_o \alpha \right) InP \tag{2.29}$$

A plot of g versus ln P gives a straight line graph whose slope is (g_m RT/$q_o\alpha$), from which q_o can be calculated.

For liquid adsorbates, the Temkin isotherm model is as follows.

$$q_e = \left(\frac{RT}{b_T} InK_T \right) + \left(\frac{RT}{b_T} InC_e \right) \tag{2.30}$$

The expression RT/b_T is related to the heat of adsorption, R is the gas constant (8.314 Jmol^{-1}K^{-1}), T is absolute temperature in Kelvin, b_T (Jmol^{-1}) is the Temkin isotherm constant, which expresses the variation of adsorption energy and k_T is the equilibrium binding constant corresponding to the maximum binding energy. Both k_T and b_T were calculated from the slope and the intercept of the linear plots of q_e vs InC$_e$.

2.9   Adsorption Kinetics

By analyzing the absorptive uptake of heavy metals from wastewater at different time intervals, the absorption kinetic of various modelling was studied by various. Some of these models are discussed in the following sections.

2.9.1   Lagergren pseudo first order model

This fitted to model the kinetic of heavy metal adsorption onto activated carbon. The linearity of each model when plotted whether the model suitably described the adsorption process or not.

The general expression for Pseudo first order equation model is shown as;

$$\frac{dq_t}{dt} = k_1(q_e - q_t) \tag{2.31}$$

the sorption capacities at equilibrium and at time are represented by q_e and q_t respectively and K_1 is Pseudo first order sorption rate constant in (L/min). applying boundary condition after integration, from t=0 to t=t_t snd q_t=0 to q_t=q_t, the integration form of equation becomes;

$$\log(q_e - q_t) = \log(q_e) - \left(\frac{k_1 t}{2.303}\right) \tag{2.32}$$

A plot of log (qe - qt) versus t should give a straight line, if the sorption is controlled by this model. k1 and qe can be determined from the slope and intercept of the plot, respectively. The experimental q_e should tally with the estimated one. Generally, higher values of k1 suggest greater adsorption.

The assumption with this model is that the rate of adsorption is proportional to the difference between the adsorption capacity (q_e) at equilibrium and the capacity at any time (Bernard *et al.* 2013)

2.9.2 Pseudo-second order model

The pseudo second order chemisorption kinetic rate equation as expressed as follows;

$$\frac{dq_t}{dt} = k_2 (q_e - q_t)^2 \qquad (2.33)$$

where, k2 is the rate constant of pseudo second order adsorption ($g.mg^{-1}.min^{-1}$). From the boundary conditions t = 0 to t = t and q_t = 0 to q_t = q_t, the integrated form of equation (2.33) becomes equation (2.34).

$$\frac{1}{q_e - q_t} = \frac{1}{q_e} + k_2 t \qquad (2.34)$$

This is the integrated rate law for a pseudo second order reaction. Equation (2.34) can be rearranged to obtain equation (2.35), which has a linear form.

$$\frac{t}{q_t} = \frac{1}{k_2 q_e{}^2} + \frac{t}{q_e} \qquad (2.35)$$

A plot of t/q_t versus t should give a straight line if this model is obeyed by the sorption process. From the slope and intercept of the plots, q_e and k_2 are determined, respectively. The experimental q_e should tally with the estimated one. Decrease in the values of k_2 suggests increased adsorption (Bernard et al., 2013).

The main assumptions of the pseudo-second order kinetic model is that rate limiting step is chemical sorption involving bond formation through sharing or exchange of electrons between the adsorbate and adsorbent. It also assumes that sorption follows the Langmuir equation.

2.9.3 Intra-particle and film diffusion kinetics

The basic assumption with intra-particle diffusion model according to Okafo *et al.* (2014) is that film diffusion is negligible and intra-particle diffusion is the only rate-controlling step, if the rate limiting step is the intra-particle diffusion, then the amount adsorbed at any time t, should be directly proportional to the square root of contact time, t, and shall pass through the origin. This is defined mathematically as follows:

$$q_t = k_{id} t^{0.5} \qquad (2.36)$$

where q_t (mg/g) is the amount adsorbed at time t (min) and K_{id} (mg. $g^{-1}.min^{-0.5}$) is the intra-particle rate constant. The logarithmic form of equation (2.36) is equation (2.37).

$$\log(q_t) = \log(k_{id}) + 0.5 \log t \qquad (2.37)$$

The plot of log q_t against 0.5 log.t should yield a straight line with a positive intercept for intra-particle diffusion controlled adsorption process. k_{id} is determined from the intercept of the plot. Higher values of k_{id} illustrate an enhancement in the rate of adsorption. To confirm that an adsorption process is controlled by intra-particle diffusion, the intra-particle diffusion coefficient, D_P, is usually calculated using the following equation:

$$D_P = \left(\frac{0.03 r_o^2}{t_{0.5}} \right) \qquad (2.38)$$

where 'r_o' (cm) is the average radius of the adsorbent particle and $t_{0.5}$ (min) is the time required to complete the half of the adsorption. If the calculated intra-particle diffusion coefficient (D_P) value is in the range of 10^{-11} to 10^{-13} $cm^2.s^{-1}$, then the intra-particle diffusion controls the rate limiting step and, if the calculated film diffusion co-efficient (D_F) value is in the range of 10^{-6} to

10^{-8} cm^2/s, then the rate limiting step is controlled by film (boundary layer) diffusion. The D_F values are calculated as follows:

$$D_F = \left(\frac{0.23 r_o \delta C_s}{C_L t_{0.5}} \right) \qquad (2.39)$$

where r_0 and $t_{0.5}$ have the same meaning as before, δ is the film thickness (10^{-3}cm), C_S and C_L are the concentrations of adsorbate in solid and liquid phase at time t, respectively.

2.10   Previous Works done on Metal Ions removal from Wastewater

Some investigators have studied the removal of Pb^{2+}, Cu^{2+}, Zn^{2+}, Cd^{2+}, Ni^{2+}, and Fe^{3+} from simulated waste water using activated carbon from agricultural wastes. Jaber in 2013, prepared activated carbon from Xanthium Pensylvanicum and tested its adsorption of Pb^{2+}, Cu^{2+}, Zn^{2+}, Cd^{2+}, Ni^{2+}, Co^{3+} and Fe^{3+} from Aqueous Solution. They found that the adsorption process obeyed the Langmuir isotherm and Freundlish Isotherm. The studies showed that Xanthium Pensylvanicum could be used as an alternative to remove high amount of toxic heavy metal ions from wastewater.

Amin *et al*. (2016) produced activated carbon from date palm trunk fibre, and the activated carbon was tested for the adsorption of Cu^{2+} from aqueous solution. They found that adsorption of the copper ion increased with increase in initial copper ion concentration and at 20 to 100 mg/l, however the percent removal of Cu^{2+} decreased from 31 to 23 % at higher Cu^{2+} concentration due to the saturation of sorption site at the adsorbent surface. They also found that the adsorption process could be described by the Langmuir isotherm. The monolayer adsorption capacity was found to be 23.5 mg/g.

Alazba *et al.* (2017) investigated the removal of Cu^{2+} and Pb^{2+} ions from aqueous solutions by adsorption on activated carbon prepared from date palm leaves and orange peel. They studied the effect of pH and adsorbent dosage, effect of pre-treatment and contact time on metal adsorption efficiency, effect of particle size, effect of bed height, effect of initial metal concentration, effect of flowrate. They found that the maximum efficiency of Cu^{2+} removal by raw D_P was at pH of 5 and that of Pb^{2+} by treated OP was maximal at pH 5-5.5. It was observed that both metal adsorption equilibria were established contact time of 30 mins and with increase in carbon dosage up to 0.5 g to 5-7 g and increased with increase in metal concentration from 50 to 150 mg/l.

Lee *et al.* (2016) prepared conventional NH_2-SBA-15 of rod shape by dissolving 4.0 g of Pluronic P123 in 160 g of 2.0MHCl Solution at 35 ^{o}C. The carbons were used for adsorption of Pb^{2+}, and Cu^{2+}, from Aqueous solution of their nitrate. The results obtained from their study showed that the thiol-group SBA-15 adsorbent of all the morphologies have a better affinity for Pb^{2+} and the amino group SBA-15 has a stronger affinity for Cu^{2+}. The Pb^{2+} uptake increase between pH of 2 and 6 and that adsorption capacity for Cu^{2+} increase between pH of 2 and 5. They found that the equilibrium data of Cu^{2+} adsorption fitted well to Langmuir isotherm.

Mokhlesur *et al.* (2014) produced activated carbons from oil palm and coconut shells chemical activation using phosphoric acid. Carbonization was done at 400 °C for an hour. The activated carbons were tested for adsorption of Pb^{2+}, Ni^{2+}, and Cr^{2+} from simulated waste water. Their results showed that the adsorption capacities of the activated carbons increased with increase in the initial lead concentration from 100 to 500 mg/l and with increase in temperature from 30 to 60 °C. The adsorption processes fitted well to the both Langmuir and Freundlich isotherms. The equilibrium initial concentration was varied from 40 to < 600 mg/l, pH of 5 and initial Pb^{2+}

concentration of 43 mg/l using the Langmuir isotherm and were found to be 74.6 and 19.6 mg/g for oil palm and coconuts shells activated carbons, respectively.

Musah (2011) produced activated carbon from Palm kernel shell by pretreatment carbonization in a muffle furnace at 600 ^{o}C for 5 mins and subsequent activated at 800 ^{o}C with H_3PO_4. The activated carbon was tested for removal of Pb^{2+} and Cr^{2+}. Percentage removal of the ions increased with increase in initial concentration and increased with increase in contact time and also with increase in dose of adsorbent. Percentage removal also increased with increase in pH up to a pH of 7.2, after which it decreased with further increase in pH. Amount of lead (II) ions adsorbed increased with decrease in particle size of the adsorbent. The adsorption process obeyed the Pseudo second order kinetics with intra-particle diffusion as one of the rate determining steps. The adsorption process was better described by the Langmuir isotherm than the Freundlich isotherm.Some of the reported values for monolayer adsorption capacities are rather low. Hence, there is still the need to discover other low cost raw materials that could yield carbons with much higher adsorption capacities.

CHAPTER THREE

3.0   MATERIALS AND METHOD

3.1   Materials

The major raw material used in this research work was Screwpine stem (*Pandanus senderi*), the chemical reagents used were Concentrated 0.1M H_3PO_4 and 0.1M NaOH stock solution, Sewage wastewater, distilled water, Jenway 3510 pH meter, atomic absorption spectrometer (Buck Scientific, model 210 VGP) to test for the concentration of the solution before and after sorption, Vecstar programmable muffle furnace (model LF3) was used for carbonizing samples, air drying oven (# BTOV 1423) was used for drying of samples. weighing balance (AR 3130) was used for weighing of samples.

3.2   Production of Adsorbent

Pandanus plant stem was used as a precursor for the preparation of activated carbon. The raw samples were purchased from local market of Anambra State, Nigeria. They were washed thoroughly with distilled water in order to remove impurities and air dried for seven days, then oven dried at 80 ^{o}C. They were crushed and sieved to a particle size between 1.00 – 1.70 mm and then stored for further used, according to Mohammad-Khah and Ansari (2009).

3.2.1   Carbonization without chemical activation

15 g of dried Pandanus stem powder was carbonised in an electric furnace at 600 ^{o}C for 3 hours. Thereafter, the carbonised product was repeatedly washed with distilled water so many times and subsequently oven dried at105 ^{o}C for 4 hours. The dried material was sieved to get the particles size of 1.70 mm. The adsorbent was labelled as Control Activated Carbon (CAC) and stored in an air tight container for further used.

3.2.2 Chemical activation

15 **g** of the crushed Pandanus were weighed and introduced into a two separate beakers and impregnated with activating agent of Sodium Hydroxide (NaOH) and Phosphoric acid (H_3PO_4) respectively, in a ratio of 1:1 by weight for 12 h. The impregnation was carried out at 80 ^{o}C in a hot air oven to achieve well penetration of chemical into the interior of the precursors. After impregnation, the mixture was introduced into the hot zone of a muffle furnace for carbonization at temperature of 600 ^{o}C for 3 h. The content was then removed from the muffle furnace after the set period and cooled in an open air for one hour. The resulting carbon were washed with distilled water until the pH of the filtrate was neutral. They were then dried in an oven at105 °C for 4 h, sieved to get the particles size 1.70mm. then the modified adsorbents were labelled as Sodium Hydroxide Powdered Activated Carbon (NaOH-PAC) and phosphoric acid Powdered Activated Carbon (H_3PO_4-PAC) when stored in a tight container for further used.

3.3   Characterization of Adsorbents

3.3.1   Percentage (%) yield and burn off (weight loss)

The yield of activated carbon was defined as the ratio of the weight of the resultant activated carbon to that of original precursor with both weights on a dry basis.

That is,

$$\% Yield = \left(\frac{W_1}{W_0} \right) 100 \qquad\qquad (3.1)$$

where W_0 (g) is the original weight of the material on a dry basis and W_1 (g) is the weight of the carbonaceous material after activation, washing, and drying. The weight loss (%burn off) refers

to the weight difference between the original char and activated carbon divided by the weight of the original char with both weights on dry basis.

$$\% \text{ Weight loss} = \frac{W_O - W_1}{W_O} 100 \qquad (3.2)$$

3.3.2   Pore volume

1 gram of the sample in a 10 ml measuring cylinder was transferred into a beaker containing 20 ml of deionized water and was boiled for 5 minutes. It was filtered, dried and weighed. The pore volume was determined by dividing the weight of sample by density of water, and the bulk density of all samples were calculated as the ratio of weight and volume of packed dry material (Gin *et al*., 2014).

3.3.3   Determination of % ash content

Sample was measured and taken in a crucible. It was then heated to $750^{\circ}C$ for 1hr 30mins. During this test the crucible was left open. After the required heating, the crucible was cooled in a desiccator and then weighed (Sebata *et al*., 2013).

$$\% \text{ Ash content} = \frac{W_{(dry\,ash)}}{W_{(dry\,ads)}} 100 \qquad (3.2)$$

where, $W_{(dry\,ash)}$ is the weight of dry ash (g) and $W_{(dry\,adsorbent)}$ is the weight of dry adsorbent (g). This test was repeated until constant ash content was obtained.

3.3.4 Determination of bulk density

The apparent or bulk density of each adsorbent was determined according to Norouzi *et al.* (2018) by weighing on known weight of each sample, after being dried at 105°C, was parked into a 10ml capacity graduated cylinder. The bottom of the cylinder was tapped gently on the laboratory bench top several times until there was no further diminution of the sample level. The bulk density was then calculated using the following equation.

Bulk density (g/cm^3) = wt of dry activated carbon in gram/ volume of packed dry material in cm^3.

$$\text{Bulk density } g\big/ cm^3 = \frac{W_{mat}}{V_{mat}} \tag{3.4}$$

where, W_{mat} is the weight of dry material (g) and V_{mat} is the volume of dry material (ml).

3.3.5 Moisture content

Sample was measured and taken in a petri dish. It was spread nicely on the dish. It was then heated at 105 ^{o}C for 1hr 30mins. the petri-dish was left open during the heating process. After heating petri-dish was removed, cooled in desiccator and then weighed (Salehzadeh, 2013).

3.3.6 Iodine adsorption number (IAN)

The Iodine Number was determined to access the absorptive capacity of prepared activated carbon. According to Itodo *et al.* (2010), 1-gram sample mixed with 25 ml of Iodine Solution (0.023M) in a beaker were swirled vigorously for 10 minutes and then filtered. 20 ml of the filtrate was titrated with the (01095M) Thiosulphate Solution to observe a pale yellow colour. 5 ml of freshly prepared starch indicator was added and titrated slowly until a colourless solution appeared. The procedure was carried out two more times. Another titration was performed with 20 ml of the Iodine Solution not treated with sample to serve as blank titration.

48

The Iodine Number (IAN) was calculated from the relationship:

$$IAN = \left[\frac{12.69 \times M \times (V_2 - V_1)}{D} \right]$$
(3.5)

V_1 = average titer ≡ volume of thiosulphate need to titrate against residual iodine after treatment with carbon;

V_2 = blank titer ≡ volume of thiosulphate need to titrate against iodine that is not treated with carbon;

D = adsorbent dosage i.e. mass of carbon used;

M is the molarity of standard sodium thiosulphate used ($Na_2S_2O_3.5H_2O$).

3.3.7 Determination of surface area using methylene blue number

Surface Area was determined using Langmuir Isotherm of methylene blue adsorption according to Itodo et al. (2010), in which different concentration of methylene blue was prepared ranging from 5 mg/l - 50 mg/l. 0.5 g of adsorbent was weighed into 250 ml Erlenmeyer flask, 20 ml of each methylene blue concentration was measured into the flask and it was corked. The mixtures were equilibrated for 24 hours and the amount of methylene blue adsorbed per gram of the adsorbent (Q_e) was calculated with the following equation:

$$Q_e = V \left(\frac{C_o - C_e}{m} \right)$$
(3.5)

Where Qe is metal concentrated on the adsorbent (mg/g) at equilibrium, Ce is metal concentrated in solution (mg/l) at equilibrium, Co is Initial metal concentrated in solution (mg/l), V is volume of initial metal solution used (L) and M is Mass of adsorbent used (g). And the result adsorption results were analyzed with Langmuir Isotherm; such as

$$\frac{C_e}{Q_e} = \left(\frac{1}{Q_m}\right)C_e + \frac{1}{K_m} \tag{3.6}$$

The plot of C_e/q_e vs. C_e gives a straight line with slope equal to $1/qm$, and intercept equal to $1/Kq_m$. Therefore, the Langmuir isotherm is an adequate description of the adsorption of the methylene blue onto adsorbent and The specific surface area was calculated by the following equation;

$$S_{MB} = \left(\frac{q_m \times a_{MB} \times N_A \times 10^{-20}}{M}\right) \tag{3.7}$$

Where S_{MB} is the specific surface area; q_m is the number of molecules of methylene blue adsorbed at the monolayer of fibers in mgg^{-1}.

a_{MB} is the occupied surface area of one molecule of methylene blue =197.2 Å²

N_A is Avogadro's number, 6.02 x 1023 mol^{-1}; and   M is the molecular weight of methylene blue, 373.9 g mol^{-1}.

3.4   Fourier Transform Infrared (FTIR) Analysis

The FTIR Spectral can provide valuable information about the chemical composition of the materials (Hassan *et al.,* 2001). It is most useful for identifying chemicals that are either organic or inorganic. It can be utilized to quantitate some components of an unknown mixture. The surface functional group of the activated carbon was determined at room temperature using Thermo Electron Nicolet 4700 FT-IR Spectra which has transmission percentage (%) recorded 500 – 4000 cm^{-1}. Solid samples of about 1 mg before and after activation were carried. The samples were grinded and milled with 100 mg KBr to form a fine powder. This powder was then compressed into a thin pellet under 7 tons for 5 minutes. The sample was then analyzed using and the spectrum was recorded in a spectral range of 500-4000 cm-1 (Gin *et al*., 2014).

3.5   Scanning Electron Microscope Energy Dispersive X-ray (SEM/EDX)

It is type of electron microscope that produces images of a sample by scanning the surface with a focused beam of electrons. The electrons interact with atoms in the sample, producing various signals that contain information about the surface topography and composition of the sample. The Energy Dispersive X-ray (EDX is a technique of elemental analysis associated to electron microscopy based on the generation of characteristics that reveals the presence of elements present in the specimens. (Manue *et al*., 2018).

Scanning electron microscopy (SEM) analysis were carried out on the activated carbon to study texture and the development of porosity. SEM samples of the aqueous suspension of AC were fabricated by dropping the suspension on to clean electric stubs and allowing water to completely evaporate.

3.6   Collection of Sewage Wastewater

The sewage wastewater was collected at WUPA Basin Sewage Treatment Plant, FCT-Abuja and was analyzed at Sheda science and technology complex (SHESTCO) Abuja, to determine the kind of heavy metal ions before treating with the prepared activated carbon.

Table 3.1: The analysis of sewage wastewater collected at WUPA

Parameters	The concentration of ions present in sewage
Cupper (Cu^{2+})	0.1804
Cadmium (Cd^{2+})	1.0030
Nickel (Ni^{2+})	0.1345
Lead (Pb^{2+})	0.7001
Zinc (Zn^{2+})	0.0240

3.7   Determination of Adsorptive Capacities

By using Odubiyi et al. (2012) method, on this experiment, 50mL of sewage wastewater sample containing mixed metals of 0.7001 mg/L Pb^{2+} and 0.1345 mg/L of Ni^{2+} and pH of 6.27 were added to a calculated amount of adsorbent, 0.6 g in a 50 mL shake flask. The pH adjustment of the solution was done using 1.0M NaOH or 1.0M H_3PO_4. The adsorbent in solution was agitated in mechanical shaker at a speed of 150 rpm at 27 ^{o}C. Blank solutions were treated similarly without the adsorbent and under control condition. The solution was filtered using a filter paper, and analyzed for the residual concentration of metals in the filtrate by atomic absorption spectrophotometer (AAS).

The amount of adsorption at equilibrium, q_e (mg/g) was calculated as follows

$$q_e = \left[\frac{C_o - C_e}{W}\right]V \qquad (3.8)$$

C_o and C_e (mg/l) are the liquid-phase concentration of wastewater at initial and equilibrium, V (L) is volume of the wastewater and W (g) is weight of the activated carbon

The percentage metal removal was calculated as follows;

$$\% \text{ Metal removal} = \left(\frac{C_O - C_e}{C_e}\right)100 \tag{3.9}$$

3.7.1 Effect of temperature

The effect of temperature on the adsorption process was examined varying the adsorption temperature at 30, 40, 50 and 60 ^{o}C. For each experiment, 50 ml of solutions were contacted with 0.6g of absorbent. Each sample was then agitated for 80 min at 150 rpm. The solution was then filtered and filtrate was analyzed.

3.7.2 Effect of contact time

The contact time between the solution and the adsorbent was performed by contacting 0.6 g of the adsorbents with 50 ml of the solution for 20 – 120 min, at pH of 6.27. the samples were removed from the rotary shaker and filtered. The filtrate was analyzed.

3.7.3 Effect of dosages

50 mL of solution were contacted with different masses of adsorbent (0.2, 0.4, 0.6 and 0.8). the pH was maintained at 6.27 and each samples were then agitated for 80 min at 150 rpm. The sample were filtered and the concentration were then analyzed.

3.7.4 Effect of pH

The effect of pH on the amount of adsorbent was analyzed between the pH range of 2, 4, 6, 8, 10. 50 mL of solution was transferred into a stoppered conical flask containing 0.6 g of adsorbent. The mixing was agitated at 150 rpm at room temperature for 24 hours. The samples were filtered and was analyzed.

3.8 Adsorption Isotherm Study

The equilibrium adsorption is fundamental in describing the interactive behavior between adsorbate and adsorbent, and it is important in the design of adsorption systems in wastewater.

3.8.1 Langmuir isotherm

The linear form of Langmuir equation is;

$$\frac{1}{q_e} = \frac{1}{K_a q_m C_e} + \frac{1}{q_m}$$
(3.10)

Where K_a is binding constant to the adsorption energy and q_m is the sorbent binding capacity, that is, the maximum sorption upon complete saturation of adsorbent surface. K_a and q_m values are calculated from the slope and intercept of the plot of Inq_e and InC_e.

3.8.2 Freundlich isotherm

Freundlich equation gives a description of adsorption data over a restricted range of concentration, and is suitable for a multilayer adsorption. The linear form of Freundlich equation is;

$$In(q_e) = In(K_f) + \frac{1}{n} InC_e$$
(3.11)

Where K_f is a constant indicating the adsorption capacity and n is adsorption intensity and can be calculated from the slope and intercept of the plot of Inq_e against InC_e.

3.8.3 Temkin isotherm

The linear form of Temkin Isotherm is given as;

$$q_e = BInA + BInC_e$$
(3.12)

where A (l/g) is maximum binding energy and B (J/mol) is heat of sorption. The value of A and B can be calculated from the slope and intercept of plot of q_e against InC_e.

3.9 Kinetic Study

The kinetic experiments for adsorption processes were also carried out by the batch process at pH 6.27. In the process, 0.6 g of adsorbent was added to 50 mL of adsorbate solutions and mixed at a constant agitation speed of 150 rpm. Samples were collected at time interval (20, 40. 60, 80, 100, 120 min) filtered and analyzed for residual metal concentration. (Sebata *et al*., 2013).

Lagergren Pseudo first and second orders models, and Intra-particle and film diffusion model were used in this to study the data analysis kinetics.

<div align="center">

CHAPTER FOUR

</div>

4.0   **RESULT AND DISCUSSION**

4.1   **Characterization of Adsorbents**

The properties of the adsorbents determined include the ash content, pH, moisture content, bulk density, surface area, iodine adsorption number, pore volume, percentage weight yield and percentage weight loss.

4.1.1   **Characterization of adsorbents produced using different activating agents**

Table 4.1a shows the effect of different activating agents on these properties for Pandanus Senderi Stem (PSS) adsorbent.

Table 4.1a: Effect of activating agents on properties of Pandanus Senderi stem plant.

Parameter	NaOH-PAC	H_3PO_4-PAC	Control
Ash content (%)	17.622	13.095	11.663
pH	6.550	7.150	6.460
Moisture Content (%)	4.382	0.994	7.784
Bulk density (g/cm^3)	0.444	0.316	0.354
Surface Area (m^2/g)	112.99	48.622	49.225
IAN	69.360	140.982	118.364
Pore Volume	1.148	1.383	1.346

Table 4.1b: Characteristics of activated carbon compared with the literature reviewed.

Parameters	Unmodified AC (CAC)	H_3PO_4-PAC	Modified AC (NaOH-PAC)	Reference activated carbon modified between 400^OC to 800^OC
Bulk density (g/cm^3)	0.354	0.316	0.444	0.458 (Ademiluyi et al., 2016).
% Ash Content	11.663	13.095	17.622	4.67-6.17 (Musah 2011)
pH	6.460	7.150	6.550	6.85 (Shanmugam et al., 2009)
% Moisture Content	7.784	0.994	4.382	1.85 (Shanmugam et al., 2009)
Pore Volume (cm^3)	1.346	1.383	1.148	1.031 (Ademiluyi et al. 2009).
Surface Area (m^2/g)	49.225	48.622	112.99	13.579-18.170 (Itodo et al. 2010)
IAN (mg/g)	118.364	140.982	69.359	1160 (Madu et al, 2013)

Table 4.2: Percentage weight yield and weight loss

Parameter	Values
% weight Yield	50.6691
% Weight Loss	49.3310

The values 112.99, 48.622 and 49.225 (m^2/g) in Table 4.1a are the results of surface area of NaOH-PAC, H_3PO_4-PAC and CAC respectively, which was determined using methylene blue adsorption by Langmuir Isotherm method. The Langmuir Isotherm showed that the amount of Methylene blue adsorbed increases as the concentration increase. Adsorption will increase with increasing methylene blue concentration. The modified activated carbon (NaOH-PAC) proves to have a higher surface area (S_{MB} = 112.99 m^2/g which compared more to that of the unmodified activated carbon (CAC), (S_{MB} = 49.225 m^2/g and least H3PO4. The trends therefore, imply that the level of accessible area of solid surface (Pandanus carbon) per unit mass of material (methylene blue dye) follows the order of: NaOH-PAC > CAC>H3PO4-PAC. It can be seen from the table 4.1a that activation of the raw pandanus stem resulted in increased surface area when treated with NaOH with a decreased in pore volume and decreased when treated with H_3PO_4 with increased in pore volume. The NaOH-PAC has possessed the highest ash content and bulk density whereas the bulk density of H_3PO_4-PAC has least pore volume. The increase in surface area of NaOH-PAC could be attributed to the destruction of the aliphatic and aromatic species present in the raw material by the activating agents leading to swift removal of volatile matters during the activation process, according to Ibrahim *et al.* (2006). These volatile matters include considerable organic by-products and minerals present in the activated carbon surface.

The reduction of the volatile matter in the activated carbons creates a high percentage of calculated ash since the ash is non-volatile (Abia *et al*., 1995). The decrease in pore volume of the carbons causes an increase in weight of the carbon to occupy more space thereby leading to increase in bulk density.

The characteristics of activated carbon made from Pandanus plant in Table 4.1b, can be observed to follow the properties within the limit of the reference activated carbon**.** The activated carbon produced in this work had acceptable properties and compared favorably with reference activated carbon which is an indication of quality of adsorbent that can be used for both liquid and gaseous purification on operations. Table 4.1b also showed that the IAN of unmodified activated carbon is 118.364mg/g, which was found to decease to 69.359mg/g after the modification process with NaOH and increased to 140.982mg/g. Nevertheless, the activated carbon has the percentage recovery and percentage burn off 50.66905 and 49.33095 respectively in Table 4.2.

4.2.   Fourier Transform Infrared (FT-IR) Analysis

Fourier Transform Infrared (FTIR) Spectra: Oxygen containing surface functional groups plays important role in influencing the surface properties and adsorption behavior of activated carbons. These groups can be formed during activation process or can be introduced by oxidation after preparation of activated carbon. The FTIR spectra obtained for the prepared activated carbon

are given in Figure 10. The spectra show that the surface functional groups of the activated carbon exhibit significant differences on the intensity of the bands detected
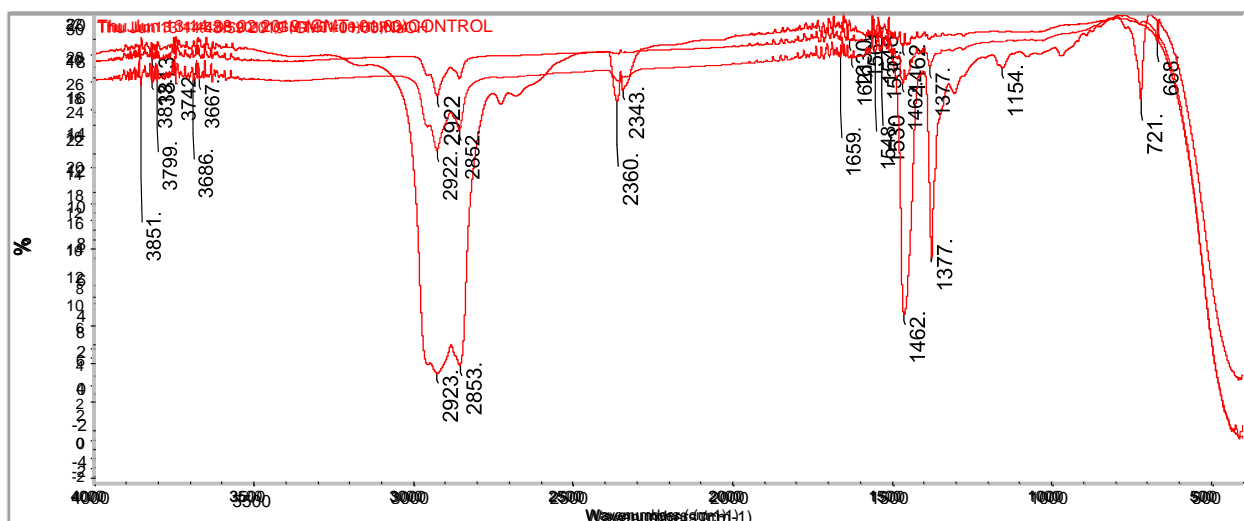
Figure 4.1: Superimposed FTIR spectrum of CAC, NaOH-PAC and H$_3$PO$_4$-PAC

In Figure 4.1, the band indicates the presence of O-H alcoholic group which was observed at the absorption around 3813.98 cm^{-1}. a strong and broad adsorption peak appeared at 2923.39 – 2852 cm^{-1}, which corresponds to the C-H functional group and this shows the presence of methyl group sp^3 in the raw sample. There was another weak peak observed around 2360.52 – 2343.44 cm^{-1}, corresponding to the O-H showing the presence of phenol group. the band located at 1561.79cm^{-1} corresponds the presence of C=C showing the presence of aromatic carbon. Another peak was observed around 1462.40 and 1377.01cm^{-1}, corresponding the presence of (= - CH$_3$). A subsequent small rise at 1154.30 cm^{-1} could be assigned to the stretching of C-O is esters. The peak at 721.61 cm^{-1} indicate the presence of (-C-H). It can be suggested from the spectrum that the main oxygen groups present in the CAC are methyl, aromatic and esters group. Furthermore, the CAC samples contain a lot of elements and impurities before undergoing the activation process. Unlike spectrum showed by CAC, spectrum of NaOH-PAC and H$_3$PO^4-PAC in Figure 4.11 indicates the reduction in absorption peaks of functional groups. This absorption illustrates

the presence of active carbon in the prepared samples. This further proves that the presence of active carbon might be obtained during carbonization were successfully removed, as the volatile compounds.

**Table 4.3: Superimposed FTIR spectrum of CAC, NaOH-PAC and H₃PO₄-PAC**

S/N	Functional Group (bonds)	Type of compound	Characterization adsorptions (cm^{-1})	Intensity
1	O-H	Monomeric Alcohol	3851 – 3667	Variable
2	C-H	Alkanes	2923 – 2852	Strong, stretch beading
3	O-H	Phenol	2360 – 2343	Stretch, H-bonded
4	C=C	Aromatic rings	1659 – 1530	Stretch
5	-CH₃	Methyl group	1462 – 1377	Variable
6	C-O	Presence of carboxylic acid, esters and ethers	1150 – 1050	Stretch
7	-C-H	Presence of alkynes	710 – 700	Stretching vibration

4.3 Scanning Electron Microscope Analysis

The SEM micrographs Figure-4.13 of activated carbon particles prepared from pandanus showed that when the sample is treated with activates, the opening of the pores in the rough surfaces on the prepared carbon samples occurs, due to extraction of some materials from the surface by the chemical activation (Shamsuddin *et al*., 2015). It shows that, activating agent influenced the morphological characteristics of the carbon surface. The micrograph for unmodified carbon, (Figure 4.13a) shows that the surface barely consists of pore. Among all the micrographs, surface of the activated carbon prepared by NaOH agent shows the presence of pores. NaOH impregnated activated carbon (Figure 4.13b) clearly showed partially developed honey-comb like highly defined pores and cavities than unmodified carbon. However, the pores are non-uniform. On the other hand, activated carbon impregnated with H_3PO_4 (figure4.13c) do not show much pores structure. Pore structures of activated carbon prepared using different activating agents point to the occurrence of different reaction mechanisms. The mechanisms by which H_3PO_4 activates an existing carbon are more complex and involves the disintegration of structure following intercatalation as well as some gasification whereas activation with NaOH promotes the extraction of water molecules from lignocellulogic materials leading to the generation of porosity (Marsh, 2006).

Greater amount of minerals like Calcium, Silver, Potassium Silicon, Phosphorus, Aluminum, Magnesium and Sodium are naturally present in pandanus stem. However, Calcium constitutes between 15 – 20% of weights of all minerals in Pandanus stem. The EDX spectrum indicated that carbon content of the CAC is 82.51% where as carbon content of the NaOH-PAC and H_3PO_4-PAC are 84.42 and 86.38 % respectively. Indication of aluminum and silver in the EDX

spectrum might have been due to environmental pollution (Fung *et al*., 1999) and normally present in the stem.
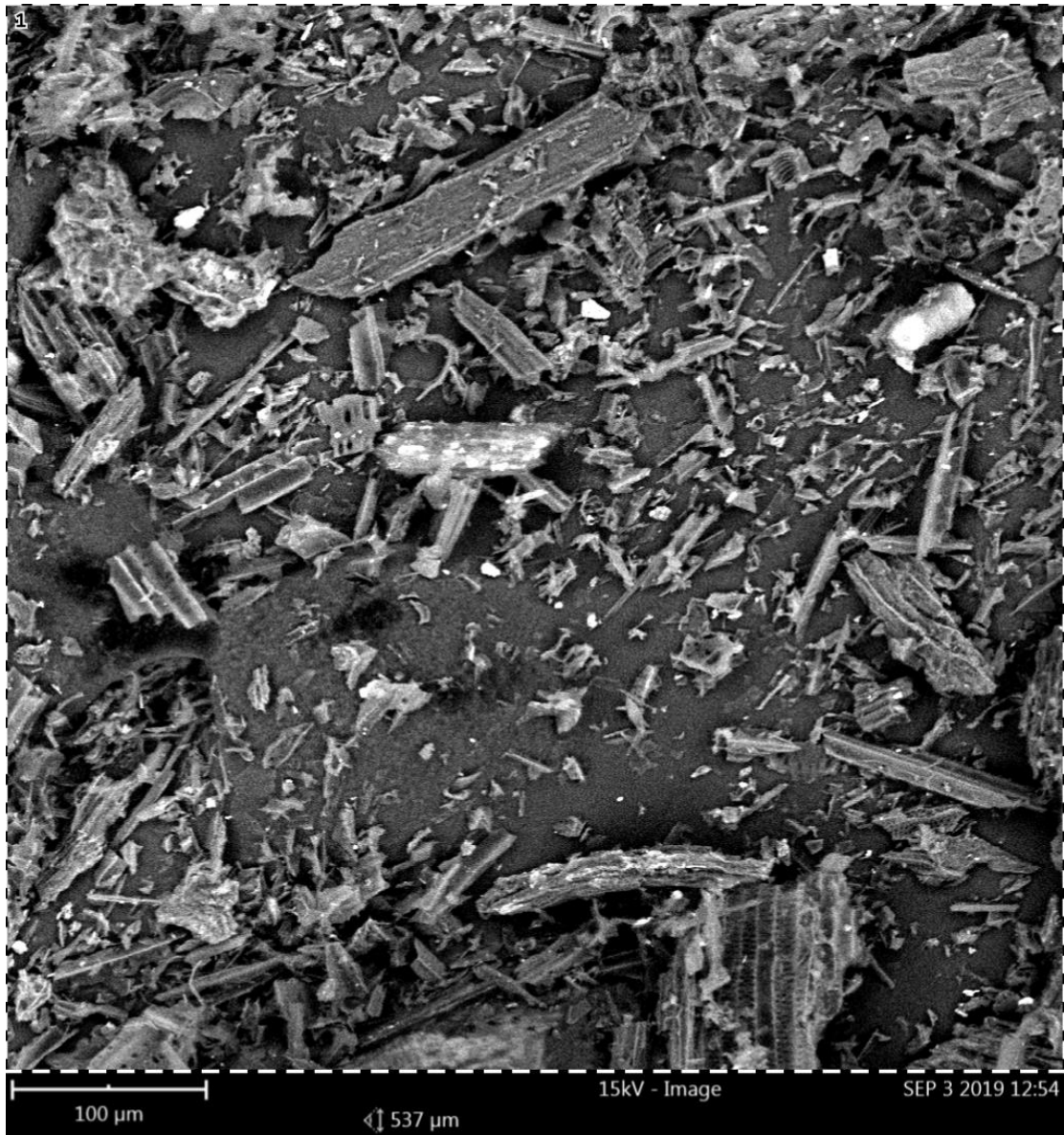
Figure 4.2a: The micrograph of CAC SEM image
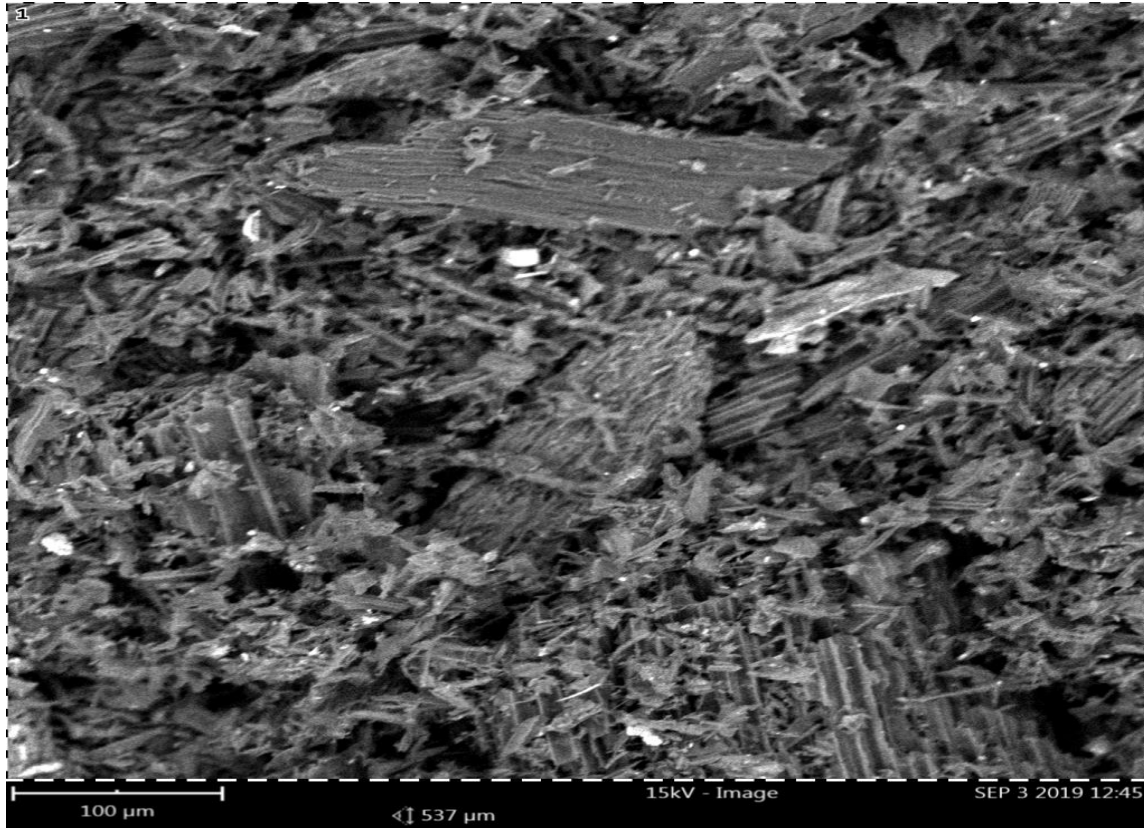
**Figure 4.2b: Micrograph of NaOH-PAC SEM image**

Figure 4.2c: Micrograph of H$_3$PO$_4$-PAC SEM Image
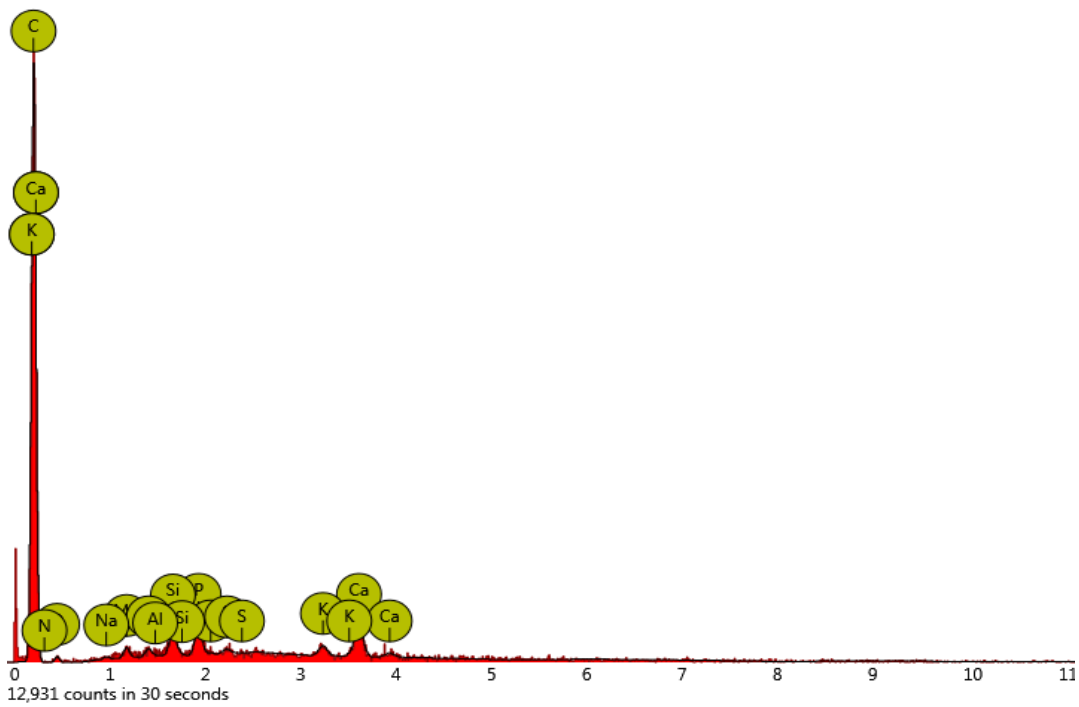
Table 4.4a: EDX Result on CAC

Element Number	Element Symbol	Element Name	Atomic Conc.	Weight Conc.
6	C	Carbon	90.96	82.51
8	O	Oxygen	3.36	4.06
20	Ca	Calcium	1.06	3.22
47	Ag	Silver	0.31	2.50
7	N	Nitrogen	1.75	1.85
19	K	Potassium	0.47	1.38
14	Si	Silicon	0.63	1.35
15	P	Phosphorus	0.50	1.16
13	Al	Aluminium	0.32	0.65
16	S	Sulfur	0.26	0.63
12	Mg	Magnesium	0.31	0.57
11	Na	Sodium	0.07	0.13
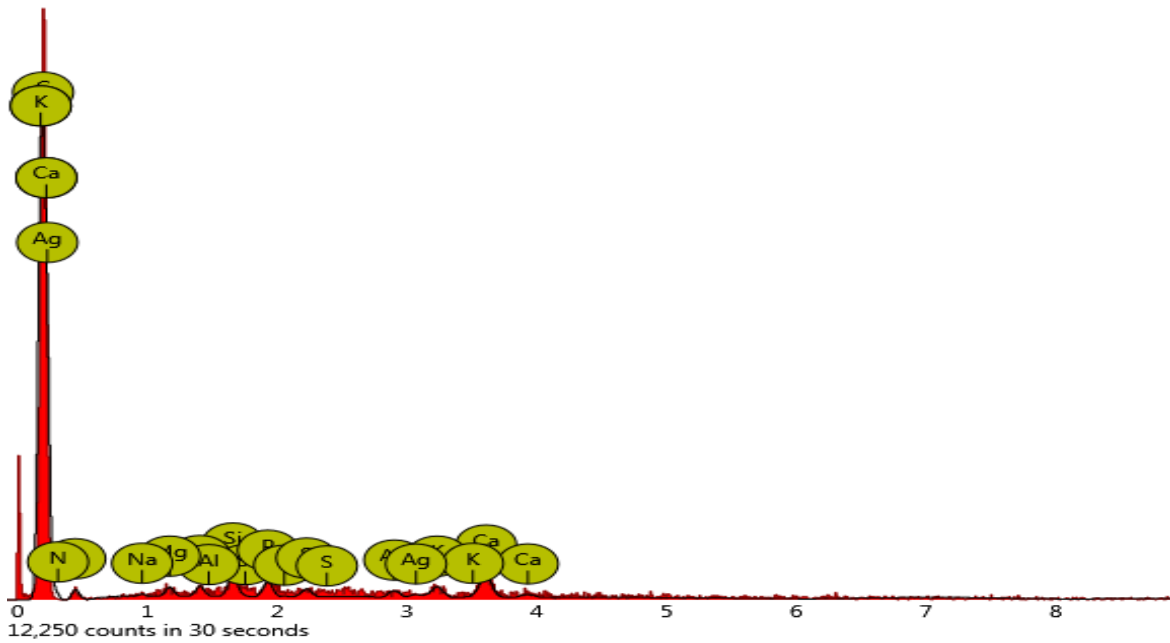
Figure. 4.4b: EDX Graph of CAC

Table 4.4c: EDX of H$_3$PO$_4$-PAC

Element Number	Element Symbol	Element Name	Atomic Conc.	Weight Conc.
6	C	Carbon	93.18	86.38
20	Ca	Calcium	1.30	4.02
8	O	Oxygen	1.88	2.32
15	P	Phosphorus	0.85	2.03
14	Si	Silicon	0.70	1.52
19	K	Potassium	0.38	1.15
7	N	Nitrogen	0.94	1.01
12	Mg	Magnesium	0.31	0.58
13	Al	Aluminium	0.22	0.46
16	S	Sulfur	0.14	0.36
11	Na	Sodium	0.10	0.18

12,931 counts in 30 seconds

Fig. 4.4d: Graph of EDX H$_3$PO$_4$-PAC

Table 4.4e: EDX result of NaOH-PAC

Element Number	Element Symbol	Element Name	Atomic Conc.	Weight Conc.
6	C	Carbon	91.44	84.42
20	Ca	Calcium	1.34	4.12
8	O	Oxygen	3.08	3.79
14	Si	Silicon	0.75	1.63
15	P	Phosphorus	0.66	1.56
7	N	Nitrogen	1.34	1.45
19	K	Potassium	0.26	0.79
12	Mg	Magnesium	0.42	0.78
13	Al	Aluminium	0.29	0.60
11	Na	Sodium	0.25	0.45
16	S	Sulfur	0.17	0.42

12,931 counts in 30 seconds
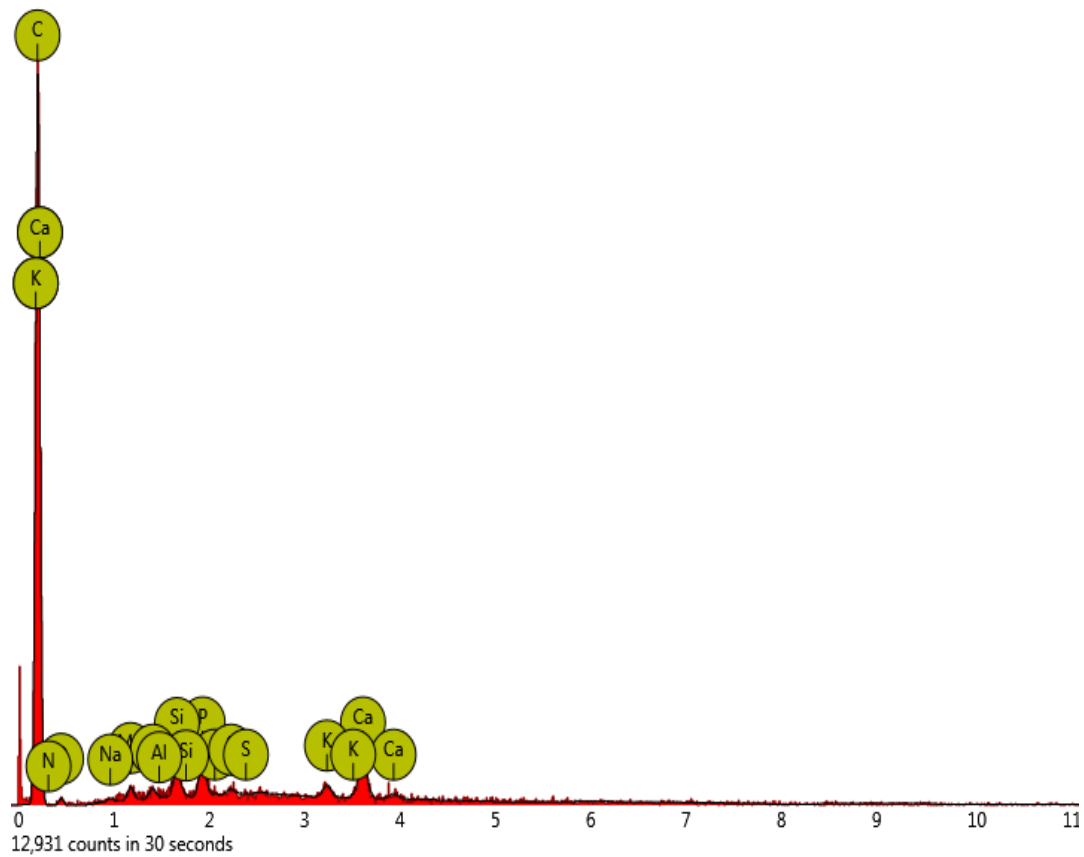
Figure. 4.4f: Graph of EDX NaOH-PAC

4.4   Effect of Process Variables on Adsorption

4.4.1   Effect of pH on adsorption

Figure 4.4 shows the effect of pH of the metal solutions on the adsorption of the metals by the carbons. The results are also presented in tabular for in Appendix for Pb^{2+} and Ni^{2+} adsorption.
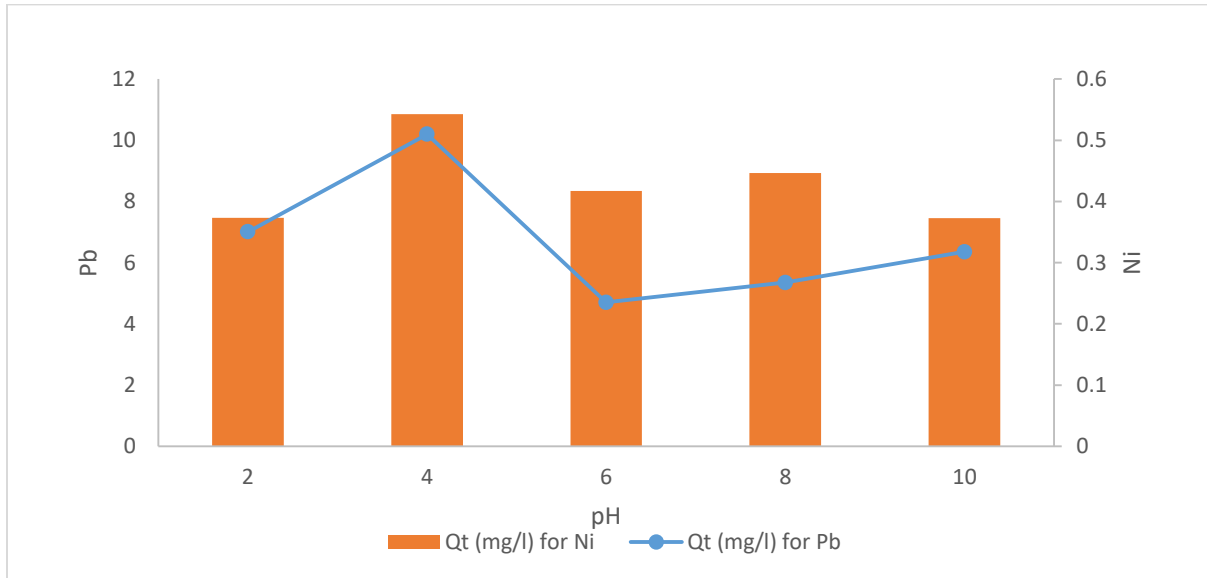
Figure 4.4a: Effect of pH on metal ions adsorption capacity
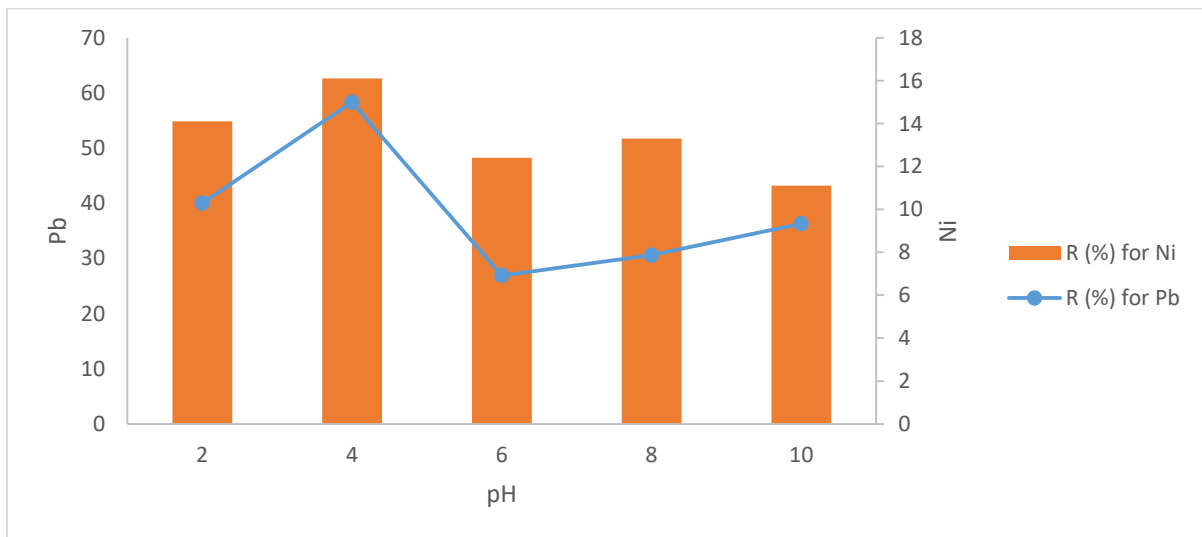
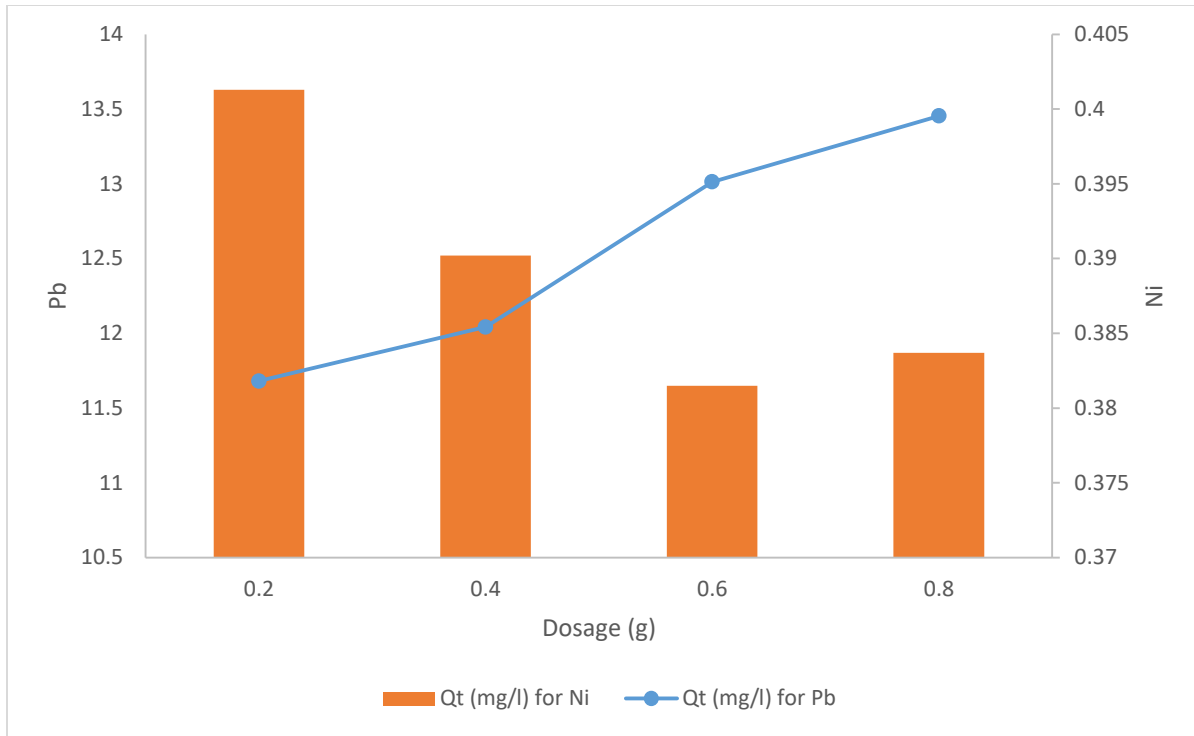**Figure 4.4b: Effect of pH on percentage metal removal**

The effect of pH on the adsorption and % metal removal Pb^{2+} and Ni^{2+} by NaOH-PAC adsorbent was examined by vary the solution pH from 2.0 – 10.0 using initial metal ion concentration at temperature of 25. Figure 4.4a and 4.4b displayed the variation of solution pH on the sorption capacity and percentage metal removal from the solution by the adsorbents. The optimum value of pH for Pb^{2+} and Ni^{2+} at 10.197 mg/g and 0.4013mg/g adsorption capacity is 4. It is also observed that the uptake (% removal) of the metal ions depends on pH where optimal metal removal efficiency of both Pb^{2+} and Ni^{2+} occurred at a pH 4.0.

Percentage removal for Pb^{2+} increased from 40 to 58.3% for pH increase from 2.0 – 4.0 and decreased to 26.9 at pH 6 and further increased to 30.6%, while the % removal for Ni^{+} increased from 14.4 to 16,1% for pH increase from 2.0 – 4.0 and decreased to 12.4 at pH 6 further increased to 13.3% at pH with further decrement 11.1% at pH 10.

The plot show that the amount of metal ions removed from the solutions by the adsorbents increased as the pH from 2.0 – 4.0 for Pb and Ni. This shows that the optimum pH for the sorption is 4. The decrease in uptake at higher and lower pHs may be attributed to the formation of precipitates of the metal hydroxides at higher pH and the formation of more H^{+} ions at lower pH, which might compete with the metal ions for active sites on the adsorbent surface (Onwu and Ogah, 2010).

4.4.2   Effect of adsorbent dosage on adsorption

Figure 4.5 shows the effect of dosage of the adsorbents used on the adsorption of the metals from their solution. The results are also presented in tabular form in appendix for Pb^{2+} and Ni^{2+} adsorption.

Figure 4.5a: Effect of Dosage on metal ions adsorption capacity
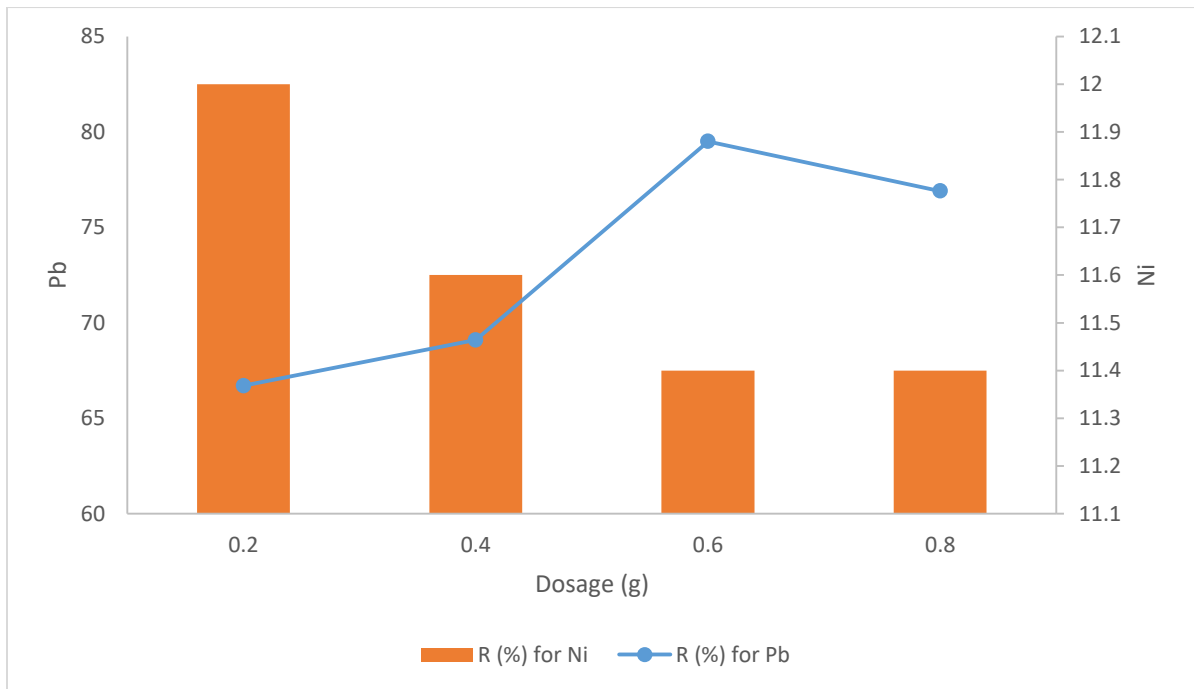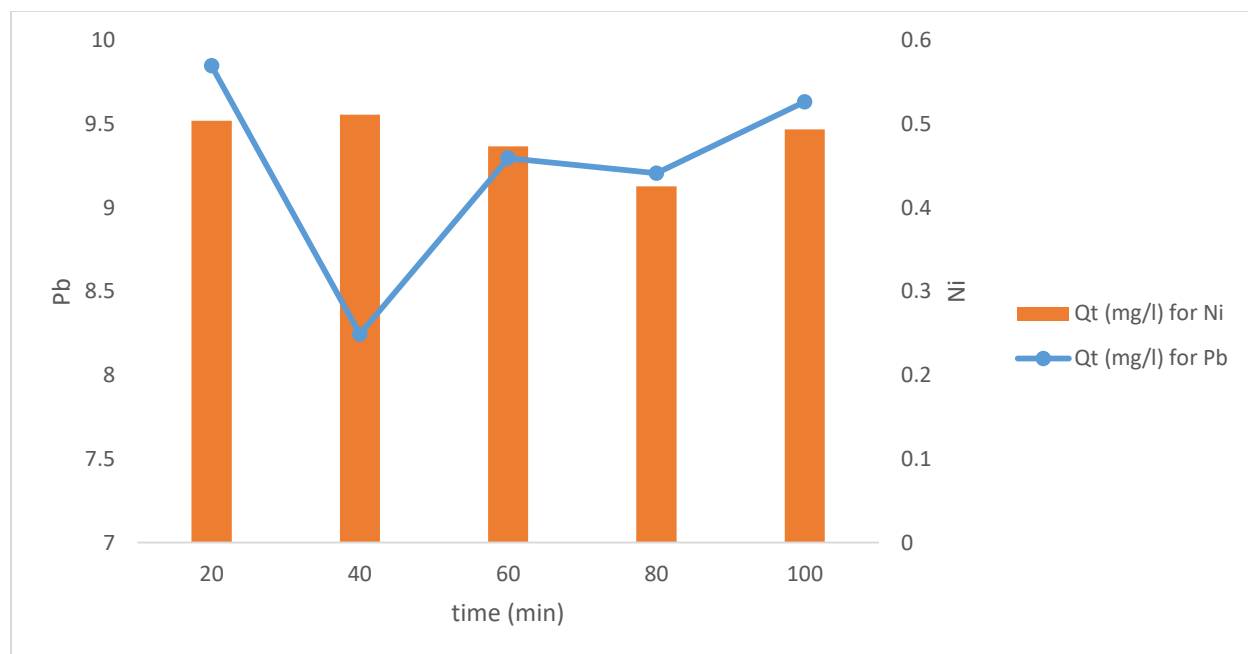

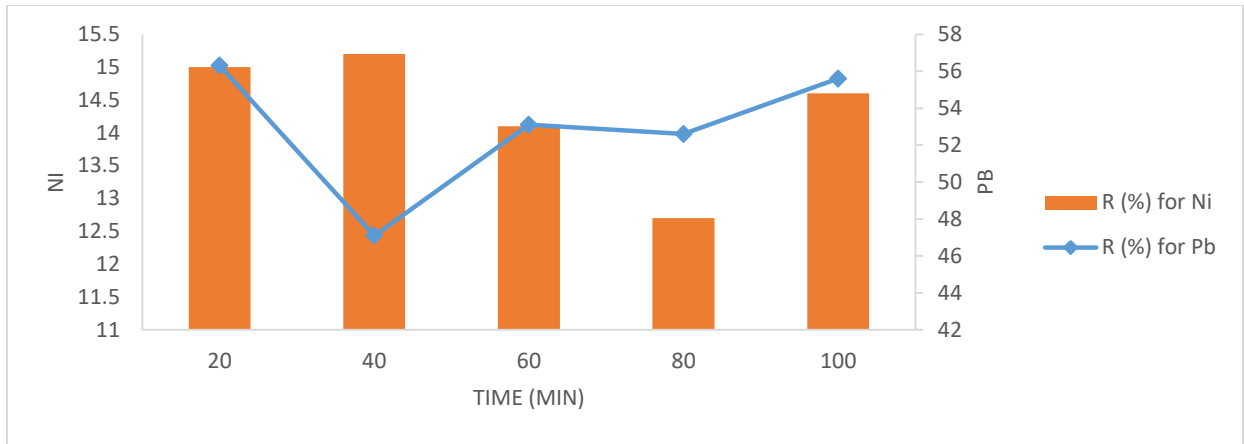**Figure 4.5b: Effect of Dosage on percentage metal removal**

The effect of adsorbent dosage on metal adsorption capacity and percentage metal removal are shown in Figure 4.5a and 4.5b. a trend on increment in adsorption capacity and metal removal with increment in adsorbent dosage was observed from 0.2 – 0.6 g for Pb^{2+} and decrement was observed throughout in Ni^{2+}. Adsorbent recorded a maximum capacity of 13.45mg/g for Pb^{2+} and 0.4013mg/g for Ni at 0.8 g for Pb^{2+} and 0.2 g for Ni^{2+}. The metal increment in adsorption capacity with increase in adsorbent dosage in Pb^{2+} was expected, since number of adsorbent particles increases and thus more surface areas were available for metals attachment.

4.4.3   Effect of contact time on adsorption

Figure 4.6 shows the effects of contact time on the adsorption of Pb^{2+} and Ni^{2+} using NaOH-PAC. The results are also presented in tabular form in Appendix.

**Figure 4.6a: Effect of contact time on metal ions absorption capacity**

Figure 4.6b: effect of contact time on percentage metal removal

The relationship of percentage metal removal by adsorption with contact time was plotted and presented in Figure, 4.6. there is variation in amount of the adsorbed metal ions for both metal

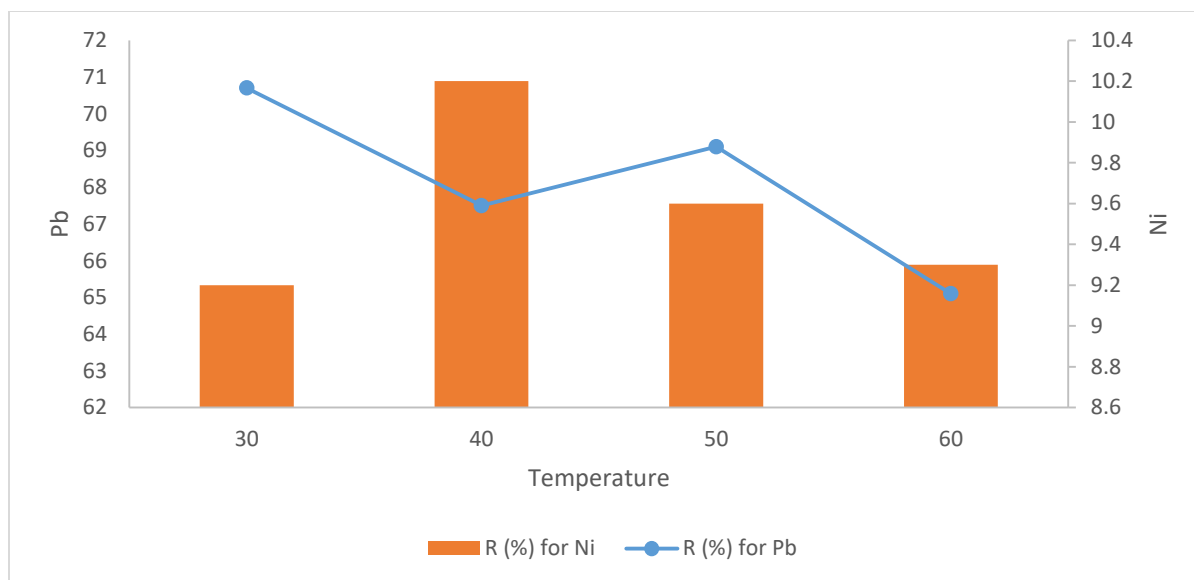### 4.4.4 Effect of adsorption temperature

Figure 4.7 shows effect of adsorption temperature on the adsorption of the metals by the carbons. The results are also presented in tabular form in table are in appendix.
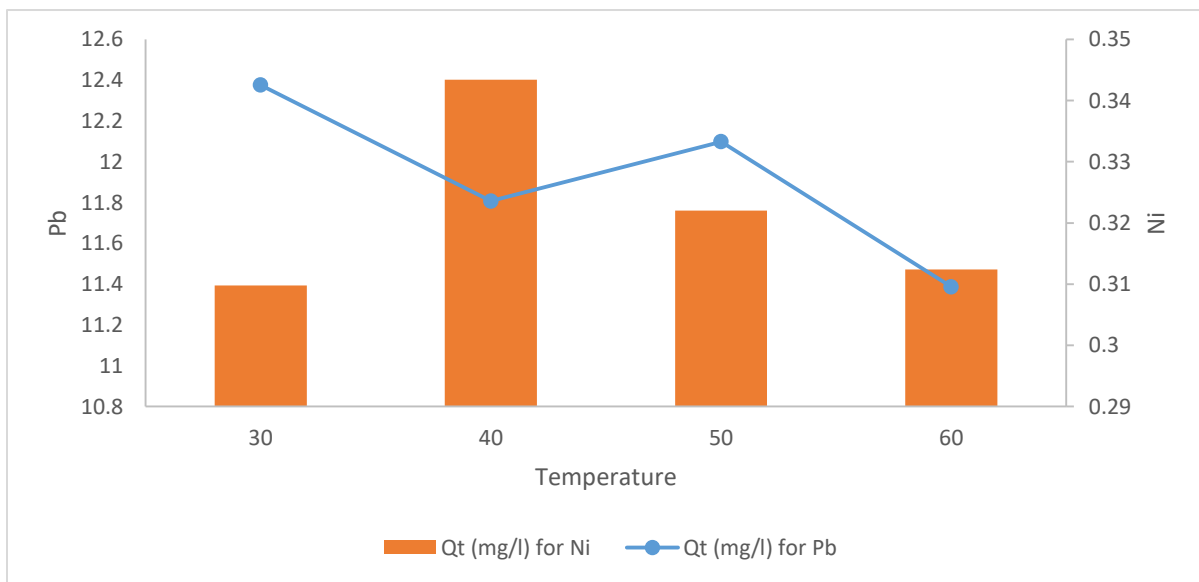
Figure 4.7a: Effect of adsorption temperature on metal ions absorption capacity

Figure 4.7b: Effect of adsorption temperature on percentage metal removal

The effect of temperature on the adsorption of metal ions of Pb and Ni was evaluated by varying the temperature from 20 – 80 $^{\circ}$C, and the plot on Figures 4.4a and 4.4b show that as the temperature increases, the adsorption capacity varying for both metal while the % metal removal shows a slightly decrease in Pb as temperature increase and also show a little constant variation on Ni.

4.5 kinetic Studies

In order to investigate the kinetics of the adsorption process, the data show in Figures 4.6 – 4.7 were analyzed using the kinetic model equations, where are Pseudo-first order, Pseudo-second order kinetic model equations. The mathematical linear forms of the equation were used.

The associated kinetic parameters for each of the kinetic models for the different metal concentration have been evaluated from the slopes and intercepts of the respective linear plots and are shown in Tables 4.5 and 4.6

Table 4.5: The kinetic parameters for Pb^{2+} adsorption on NaOH-PAC

Kinetic Model	Parameters	Solute concentration (mg/l) at 0.7001 mg/l
Pseudo first Order	K_1 (min^{-1})	0.8883
	Q_e (mg/g)	0.994
	R^2	0.3474
Pseudo second Order	K_2 (g.mg^{-1}.min^{-1})	0.043
	Q_e (mg/g)	14.728
	R^2	0.9959
Intra-particle diffusion	K_{id}	8.688
	R^2	0.8603

A comparison of the various kinetic plots based on their linear regression coefficient (R^2) values and having compared experimental and predicted value, second order fitted the adsorption. Table 4.5 indicates that the adsorption process follows the second order rate expression. The adsorption of Pb^{2+} on NaOH-PAC carbon can best be described using the pseudo-second order model. R^2 value of the second order kinetic equation is obtained as 0.9959. the regression coefficient is high. Therefore, the kinetic of adsorption is explain by the second order, because the regression coefficient for first order is 0.3474, while the regression coefficient of second order is greater, 0.9959. On the other hand, when the Qe values obtained from the equilibrium are compared, the second order kinetic equation predicts closer result than the first order, the Qe value estimated by the experimentally obtained Qe=12.3753 mg/g (Kilic *et al.*, 2017). It is

therefore assuming that the rate limiting step in the adsorption process maybe chemical adsorption, in order word, chemisorption.

Table 4.6: The kinetic parameters for Ni^{2+} adsorption on NaOH-PAC

Kinetic Model	Parameters	Solute concentration (mg/l) at 0.1345
Pseudo first Order	K_1 (min^{-1})	-0.2475
	Q_e (mg/g)	0.9811
	R^2	0.1588
Pseudo second Order	K_2 (g.mg^{-1}.min^{-1})	1976.7
	Q_e (mg/g)	0.2983
	R^2	0.9476
Intra-particle diffusion	K_{id}	0.492
	R^2	0.8327

A comparison of the various kinetic plots based on their linear regression coefficient (R^2) values and having compared experimental and predicted value, second order fitted the adsorption. Table 4.6 indicates that the adsorption process follows the second order rate expression. The adsorption of Ni^{2+} on NaOH-PAC carbon can best be described using the pseudo-second order model. R^2 value of the second order kinetic equation is obtained as 0.9476. The regression coefficient is high. Therefore, the kinetic of adsorption is explain by the second order, because the regression coefficient for first order is 0.1588 while the regression coefficient of second order is greater, 0.9476. On the other hand, when the Qe values obtained from the equilibrium are compared, the second order kinetic equation predicts closer result than the first order, the Qe value estimated by the experimentally obtained Qe=0.3434 mg/g (Kilic *et al*., 2017). It is

75

therefore assuming that the rate limiting step in the adsorption process maybe chemical adsorption, in order word, chemisorption.

4.6 Isotherm Studies

The isotherm data obtained for the adsorption process were analyzed using Langmuir, Freundlich and Temkin Isotherms.

4.6.1 Isotherm study of Pb^{2+} and Ni^{2+} adsorption on NaOH-PAC

The isotherm data obtained for the adsorption of Pb^{2+} and Ni^{2+} on NaOH-PAC are shown in table from which the Langmuir, Freundlich and Temkin Isotherm for the adsorption process was obtained and are show in appendix.

From Table 4.7, a comparison of the isotherms based on their linear regression coefficient (R^2) values shows that the Freundlich isotherm gave the best fit for the adsorption process with R^2 value of 0.9986. the calculated separation factor (1/n) has a value 2.110, this value is less than zero. This shows that during the process of absorption, at higher temperature, desorption is taking place. The behavior was reported by Rani and Sud (2015).

The Freundlich isotherm describes the equilibrium of an adsorption system where the adsorption surfaces are heterogeneous. Hence the surface does not assume monolayer characteristics. As compared to the Langmuir model and Temkin.

The adsorption capacity was found to be 5.848 mg/g which is higher than the values obtained for activated carbon from some other raw materials such as bamboo dust with value of 2.151mg/g (Kannan *et al*., 2009), coconut with values of 4.38mg/g and seed hull of palm tree with value of 3.77mg/g (Gueu *et al*., 2007).

Table 4.7: The Isotherm Parameters for Pb^{2+} adsorption on NaOH-PAC

Isotherm Model	Parameters	Values
Langmuir Isotherm	K_L (l.mg^{-1})	-13.921
	Q_m (mg.g^{-1})	8.071
	R_L	-0.1105
	R^2	0.9947
Freundlich Isotherm	K_F (mg/g)	5.848
	1/n	2.110
	R^2	0.9986
Temkin Isotherm	K_T	0.3136
	b_T (KJmol^{-1})	242.79
	R^2	0.2851

Table 4.8: The Isotherm Parameters for Ni^{2+} Adsorption on NaOH-PAC

Isotherm Model	Parameters	Values
Langmuir Isotherm	K_L (l.mg^{-1})	-9.095
	Q_m (mg.g^{-1})	0.0308
	R_L	-0.9183
	R^2	0.9947

Freundlich Isotherm	K_F (mg/g)	4.87×10^{-10}
	n	0.104
	R^2	0.9986

Table 4.8: Contd.

Temkin Isotherm	K_T	0.0435
	b_T ($KJmol^{-1}$)	-3971
	R^2	0.9995

From Table 4.8, a comparison of the isotherms based on their linear regression coefficient (R^2) values shows that the Temkin Isotherm has higher value of R^2 (0.9995) when compared with Freundlich isotherm R^2 (0.9986), but value of Temkin Isotherm constant (b_T) is negative which made it unfavorable to the adsorption. The calculated separation factor (n) has a value 0.104, this value is less than zero, which is favorable to the adsorption.

The Freundlich isotherm describes the equilibrium of an adsorption system where the adsorption surfaces are heterogeneous. Hence the surface does not assume monolayer characteristics. As compared to the Langmuir model and Temkin model.

4.7 Thermodynamics Studies

The values of the thermodynamic parameters, entropy and enthalpy variation were calculated, and the distribution coefficient (K_D) as a function of temperature using the equation according to Eldien *et al* (2016);

$$In(K_D) = \left(\frac{\Delta S^O}{R} \right) - \left(\frac{\Delta H^O}{RT} \right) \tag{4.1}$$

K_D is the distribution coefficient (cm^3g^{-1}) defined as

$$K_D = \frac{Q}{C_e}$$ (4.2)

From the formula below, the thermodynamic studies were study, Where Qe is the maximum capacity of adsorbed per unit mass of adsorbent, mg/g; Ce is the equilibrium concentration, mg/l; R is the universal gas constant, $(8.314 \ mol.K^{-1})$; T is the absolute temperature solution and slope is ΔH the change in enthalpy

4.7.1 Determination of mean free energy

The mean free energy of adsorption (E) is the energy change when one mole of ions is transferred to the surface OF the membrane, infinity in the solution and it is calculated for;

$$E = -(2K_D R)^{\frac{1}{2}}$$ (4.3)

Table 4.9: Q_e and K_D parameters at different temperature

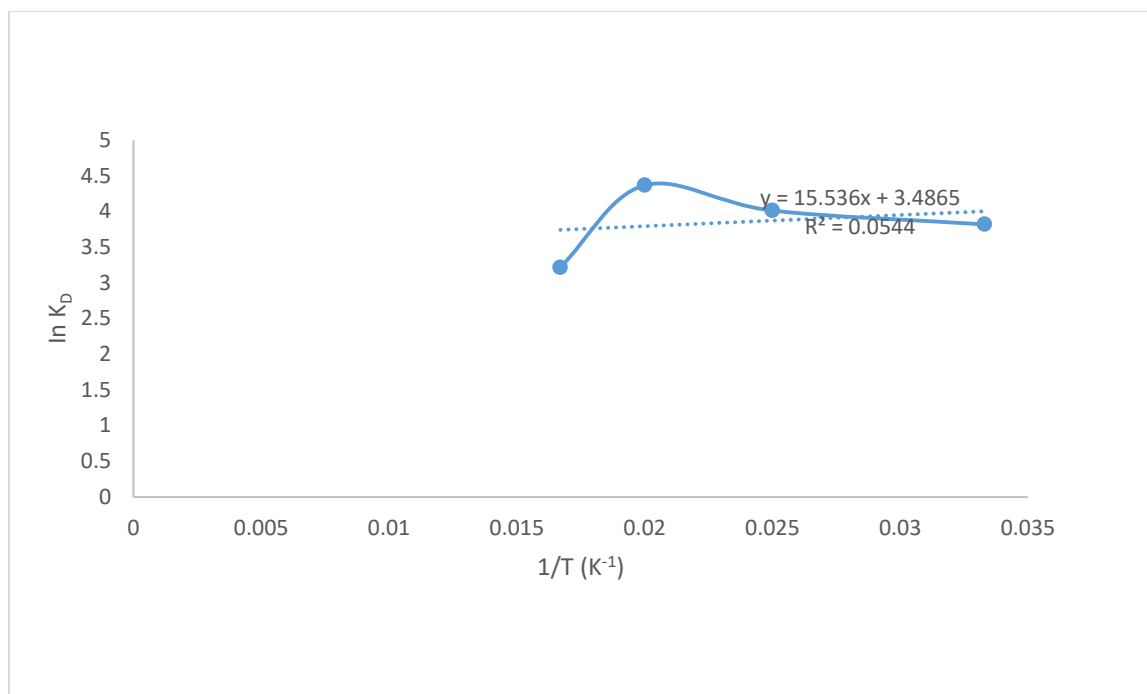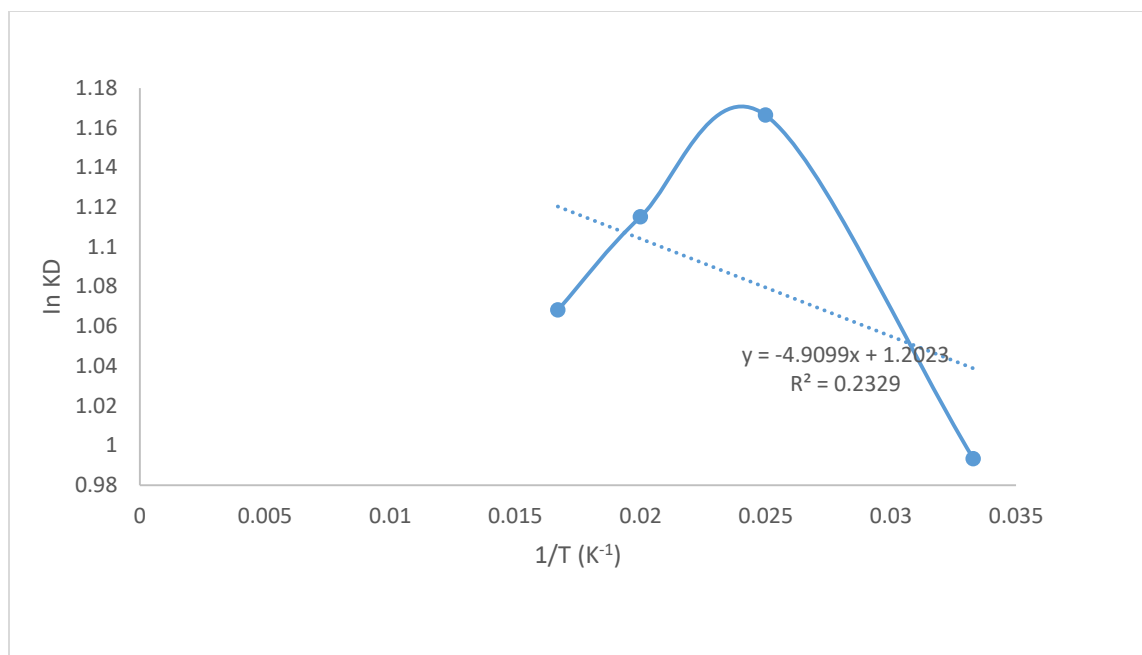| Parameters	Temperature	Q_e	C_e	K_D	In (K_D)	1/T
Pb^{2+}	30	11.3071	0.2478	45.63	3.8206	0.0333
	40	12.0588	0.2177	55.39	4.0144	0.025
	50	12.2908	0.1685	78.88	4.3679	0.02
	60	11.9271	0.4771	25.00	3.2189	0.0167
Ni^{2+}	30	0.3272	0.1214	2.70	0.9933	0.0333
	40	0.3823	0.1192	3.21	1.1663	0.025
	50	0.3683	0.1198	3.05	1.1151	0.02

| 60 | 0.3509 | 0.1205 | 2.91 | 1.0682 | 0.0167 |

Figure 4.8a: Graph of Pb^{2+} at different temperature

Figure 4.8b: Graph of Ni^{2+} at different temperature

Table 4.10: Thermodynamic parameters at different temperatures

The values of ΔH^o and ΔS^o for both Pb^{2+} and Ni^{2+} were determined from the graph, which ΔG^o were calculated from above the equation;

$$\Delta G^o = \Delta H - T\Delta S \qquad (4.4)$$

ΔH and ΔS were determined from the slope and intercept of the curve respectively as well as the calculated valves of ΔG and are listed in Table 4.10 investigating of the obtained values of the thermodynamic parameter shows that the adsorption process is endothermic. This is accordance with increasing adsorption equilibrium with increasing temperature (Eldien *et al.,* 2016).

From equation 4.3, E were calculated as follows;

Parameters	ΔH^o	ΔS^o	ΔG^o			
			30 ^{o}C	40 ^{o}C	50 ^{o}C	60 ^{o}C
Pb^{2+}	15.536	28.987	88771.87	9061.74	9351.61	9641.48
Ni^{2+}	-4.9099	9.996	3035.20	3125.16	3235.12	3335.08

Table 4.11: Free Energy at different temperatures

Parameters	Temperature	K_D	$2K_DR$	$E= -(2K_DR)^{1/2}$
Pb^{2+}	30	45.63	758.74	-27.55
	40	55.39	921.02	-30.35
	50	78.88	1316.62	-36.29
	60	25.00	415.7	-20.39
Ni^{2+}	30	2.7	44.896	-6.70

Table 4.11: Contd.

	40	3.21	53.376	-7.31
	50	3.05	50.715	-7.12
	60	2.91	48.387	-6.96

The energy of adsorption was calculated and documented in Table 4.11, the magnitude of E is useful for estimating the type of sorption reaction. Physical forces such as diffusion process may affect the sorption mechanism (Abechi *et al.*, 2018). So, the adsorption of metal ions seems to be a complex phenomenon, where diffusion and chemical bonding occur at different ranges, this may support that the monolayer capacity (q_{mas}) increase with increasing temperature.

CHAPTER FIVE

5.0   CONCLUSIONS AND RECOMMENDATION

5.1   Conclusion

Dried Pandanus stem were successfully carbonized and prepared by chemically activation using NaOH and H_3PO_4. The study observations indicate that activated carbon has been successfully prepared from Pandanus stem with a yield of 50.6691 %.

A detailed batch experimental study was carried out for the removal of Pb^{2+} and Ni^{2+} from sewage wastewater using the prepared adsorbent. This study establishes the ability of Pandanus

adsorbent to absorb high concentration of Pb^{2+} and low concentration Ni^{2+} from wastewater. The carbon adsorbent was successfully characterized by using FITR and SEM analysis.

The equilibrium of adsorption process was reached after approximately 60 min. The maximum adsorption capacity was observed at the following conditions; pH = 4.0, dosage = 0.8 and 0.4 for Pb^{2+} and Ni^{2+} respectively and temperature = 30 and 40 ^{o}C for Pb^{2+} and Ni^{2+} respectively.

Adsorption isotherm studies of Langmuir, Freundlich and Temkin were carried out for the adsorbent. Freundlich Isotherm best fitted with R^2 value of 0.9986 for both Pb^{2+} and Ni^{2+}, which also conformed to second order with R^2 value of 0.9892. The thermodynamics studies show that the reaction was endothermic in nature.

5.2   Recommendation and suggestion

Based on the excellent work covered on this research, the following recommendation and suggestion were made:

1. The adsorption column study for the process should be undertaken.

2. A different chemical reagent should be used to add value to it, in order to improve the efficiency.

3. Other heavy metal ions other than Pb^{2+} and Ni^{2+} should be used for adsorption studies using Pandanus adsorbent.

REFERENCES

Abdul, R. Y., Normirah, W., Nurshaira, H. S. and Mohd-Khairul, A. A. M. (2013). Microwave induced carbon from waste palm kernel shell activated by phosphoric acid. *International Journal of Engineering and Technology,* 5(1), 2 – 4.

Abechi, S. E. (2018). Studies of the mechanism of adsorption of methylene blue onto activated carbon using thermodynamic tools. *Science World Journal,* 13(2), 2 - 6.

Abia, A. A. and Igwe, J. C. (1995). Sorption kinetics and intra-particulate diffusivities of Cd^{2+}, Pb^{2+} and Zn^{2+} ions on maize cobs. *Afri. Journal of Biotech*, 4 (6), 509 –512.

Ademiluyi, F. T. and Nze, J. C. (2016). Multiple adsorption of heavy metal ions in aqueous solution using activated carbon from Nigerian Bamboo. *International Journal of Research in Engineering and Technology,* 10(1), 271 – 277.

Akpen, G. D., Nwaogazie, I. L. and Leton, T. G. (2011). Optimum conditions for the removal of colour from wastewater by mango seed shell based activated carbon. *Indian Journal of Science and Technology*, 4(8), 231 - 234.

Amit, B., William, H., Marica, M. B. and Mika, S. (2013). An overview of the modification methods of activated carbon for its water treatment applications. *Chemical Engineering Journal,* 219(1), 499 – 511.

Arivolia, S., Thenkuzhalib, M. and Martin, D. P. P. (2009). Application of rhodamine by acid activated carbon kinetic. Thermodynamic and equilibrium studies. *Chemical Engineering Journal,* (2), 138 – 155.

Bansal, M., Mudhoo, A., Garg, V. K. and Singh, D. (2014). Preparation and characterization of biosorbents and copper sequestion from simulated wastewater. *International Journal Environ Science Technology,* 11(1), 139 - 141.

Bernard, E., Jimoh, A. and Odigure, J. O. (2013). Heavy metals removal from industrial wastewater by activated carbon prepared from coconut shell. *International Science Congress Association*, 3(8), 3 – 9.

Buah, W. K. and Kuna, J. S. Y. (2012). Properties of activated carbon from coconut shells in Ghana. *Ghana Mining Journal,* 1(1), 51 – 55.

Debnath, S. and Ghosh, U. C. (2008). Kinetics, isotherm and thermodynamics for Cr (III) and Cr (VI) adsorption from aqueous solutions by crystalline hydrous titanium oxide. *Journal Chem. Thermodynamics*, 40(1), 67 – 77.

Eldien, I. M., Al-Sarawy, A. A., El-Halwany, M. M. and El-Msaly, F. R. (2016). Kinetic and Thermodynamic evaluation carbon derived from peanuts shell as a sorbent material. *Journal of Chemical Engineering and Process Technology*, 7(1), 20 – 25.

Gin, W. A., Jimoh, A., Abdulkareem, A. S. and Giwa, A. (2014). Production of activated carbon from watermelon peel. *International Journal of Scientific & Engineering Research*, 5(2), 66 - 77.

Gueu, S., Yao, B. and Adouby, K. (2007). Kinetics and Thermodynamics Study of Lead. Adsorption on to Activated Carbons from Coconut and Seed hull of the Palm Tree. *Int. J. Environ. Sci. Tech.,* 4(1), 11-17.

Haiyan, M., Dingguo, Z., Zaher H., Sunguo, W., Heng C. and Haiyan W. (2015). Preparation of Pinewood and Wheat Straw based Activated Carbon via a Microwave assisted Potassium Hydroxide Treatment and an Analysis of the Effects of the Microcwave Activation Condition. 2nd *International Conference on Biological and Environmental Engineering,* 2(2), 12 – 26.

Hassan, M., Al-Swaidan and Ahmad, A. (2011). Synthesis and characterization of activated carbon from Saudi Arabian dates tree's fronds wastes. *3rd International Conference on Chemical, Biological and Environmental Engineering*, 20(3), 407 - 410.

Hesas, R. H., Arash, A. N., Wan-Mohd, A. W. D. and Sahu, J. N. (2013). Preparation and characterization of activated carbon from apple waste by microwave-assisted phosphoric acid activation: Application in methylene blue adsorption. *International Journal of Applied Sciences and Environmental Management*, 8(2), 2950-2966.

Highina, B. K., Aji, M. M. and Gutti, B. (2017). Production and characterization of activated carbon (AC) from groundnut shell and its application in water treatment. *University of Maiduguri, Faculty of Engineering Seminar Series,* 8(1), 12 - 16.

Ibrahim, S. C, Hanafiah, M. A. K. M. and Yahya, M. Z. A. (2006). Removal of cadmium from aqueous solutions by adsorption onto sugarcane bagasse. *American-Eurassian J. Agric. and Environ. Sci.*, 1 (3), 179 – 184.

Itodo, A. U., Itodo, H. U. and Gafar, M. K. (2010). Estimation of surface area using langmuir isotherm method. *Journal of Applied Science and Environmental Management*, 14(4), 141-145. www.bioline.org.br/ja.

Kannan, N. and Veemaraj, T. (2009). Removal of Pb(II) ions by adsorption onto bamboo dust and commercial activated carbons – A comparative study. *Electronic Journal of Chem,* 6(2), 247-256.

Kantila, V. W., Altafhusain, B. N., Ratnakar, J. T. and Narendra, J. (2009). In-vitro regenerating plantlets in pandanus amarylifolius roxb as a model system to study the development of lower epidermal papillae. *Society for In-vitro Biology,* (45)6, 701-707.

Kilic, M. and Janabi, A. S. K. (2017). Investigation of dyes adsorption with activated carbon obtained from cordia myxa. *Bilge International Journal of Science and Technology Research*. 1(2):87 – 104.

Kwaghger, A. and Adejoh, E. (2012). Optimization of conditions for the preparation of activated carbon from mango nuts using ZnCl. *International Journal of Engineering Research and Development*, 1(2), 01-07.

Lee, J. Y., Chen, C. H., Cheng, S. and Li, H. Y. (2016). Adsorption of Pb(II) and Cu(II) metal ions on functionalized large-pore mesoporous silica. *International Journal of Environmental, Science and Technology,* 13(1), 65–76.

Luka, Y., Highina, B. K. and Zubairu, A. (2018). The promising precursors for development of activated carbon: Agricultural waste material – A review. *International Journal of Advances in Scientific Research and Engineering*, 4(1), 223 - 229.

Manue, S., Simone, B., Harpreet, K. L., Rita, B. and Elena, B. (2018). Energy dispersive x-ray microanalysis: A powerful tool in biomedical research and diagnosis. *European Journal of Histochemistry,* 20(12), 2314 – 2318. EJH. Doi:10.4081/ejh.2018.2841.

Mario, A. T. and Hiromitsu, T. (2018). Chemistry of pandanus alkaloids. *International Journey of Chemistry and Biology,* 82(1), 1-28.

Marsh, H., Fung, K. F., Zhang, Z. Q., Wongj, W. C. and Wongfluoride, M. H. (2006). Activated carbon, francisco rodriguesz reinoso, elsevier, amsterdam content in tea and soil from tea plantations and the release of fluride into tea liquor during infusion. *International Journal of Food and Agriculture*, 10(4), 27 – 31.

Menéndez-Díaza, A. and Martín-Gullón, I. (2006). Types of carbon adsorbents and their production. *International Journal of Applied Sciences and Environmental Management*, 10(2), 102-115.

Menkiti, M. C., Aneke, M. C., Ejikeme, P. M., Onukwuli, D. O. and Menkiti, N. U. (2014). Adsorptive treatment of brewery effluent using activated chrysophyllum albidium seed shell carbon. *International Journal of Chemistry and Material Science,* 3(1), 1-4. https://doi.org/10.1186/2193-1801-3-213

Mohamed, S., Jacek, N. and Andrzej, G. (2017). Low-cost adsorbents derived from agricultural by-products/wastes for enhancing contaminant uptakes from wastewater, a review. *International Journal of Environmental Studies*, 26(2), 479-510.

Mohammad-Khah, A. and Ansari, R. (2009). Activated charcoal: Preparation, characterization and application: A review article. *International Journal of ChemTech Research CODEN (USA):IJCRGG,* 1(4), 859 – 864.

Mohammed, A. A. and Sokoya, S. O. (2016). Bio-sorption of Fe (II) and Cd (II) ions from aqueous solution using a low cost adsorbent from orange peels. *International Journal of Applied Sciences and Environmental Management*, 20(3), 702-714.

Mokhlesur, M. R., Mohd, A., Alias, M. Y., Yunus, B. K. and Rezaul, H. A. (2014). Removal of heavy metal ions with acid activated carbons derived from palm and coconut shells. *International Journal of Applied Chemistry,* 7(1), 3634-3650. doi:10.3390/ma7053634

Moreno-Pirejan, J. C. and Giraldo, L. (2011). Study of activated carbon by pyrolysis of mangifera   indica seed (mango) in presence of sodium and potassium hydroxide. *E-Journal of   Chemistry*, 9(2),780 – 785.

Musah, M. (2011). Kinetic study of the adsorption of Pb(II) and Cr(III) ions on palm kernel shell activated carbon. *Journal of Chemistry and Environmental Science,* 3(10), 10 – 15.

Norouzi, S., Heidari, M., Alipour, V., Rahmanian, O. and Fazlzadeh, M. (2018). Preparation, characterization and Cr(VI) adsorption evaluation of NaOH-activated carbon produced from date press cake: An agro-industrial waste. *International Journal of Food and Agriculture*, 25(8), 48-56.

Obiora-Okafo, A., Nnanwube, A., Menkiti, M. C. and Onukwuli, O. D. (2014). Removal of particles from wastewater using locally prepared activated carbon: Equilibrium, kinetic, thermodynamic and optimization study. *Int. Journal of Engineering and Innovative Technology,* 4(1), 21 - 25.

Oboh, I. O., Aluyor, E. O. and Audu, O. K. (2009). Use of chrysophyllum albidum for the removal of metal ions from aqueous solution. *Academic Journals of Scientific Research and Essay*, 4(6), 632-635.

Odubiyi, O. A., Awoyale, A. A. and Eloka-Eboka, A. C. (2012). Wastewater treatment with activated charcoal produced from cocoa pod husk. *International Journal of Environmental and Biology*, 4(3), 162-175.

Okoroigwe, E. C., Ofomatah, A. C., Oparaku, N. F. and Unachukwu, G. O. (2013). Production and evaluation of activated carbon from palm kernel shells (PKS) for economic and environmental sustainability. *International Journal of Physical Sciences*, 8(19), 1036-1041. www.academicjournals.org/IJPS

Onwu, F. K., Sonde, C. U. and Igwe, J. C. (2014). Adsorption of Hg(II) and Ni(II) ions from aqueous solutions using unmodified and carboxymethylated granular activated carbon (GAC). *American. Journal of Physical Chemistry,* 3(6), 89-95.

Rajeshwar, M. S., Raja, R. P., Margit, V. and Imre, V. (2011). Preparation of activated carbon for the removal of Pb (II) from aqueous solutions. *Journal of Nepal Chem.* Soc., 28(1), 223 – 227.

Rani, S. and Sud, D. (2015). Effect of temperature on adsorption – Desorption behavior of triazophos in Indian soil. *Indian Journal of Sciences,* 61(2), 36-42.

Sadashiv, B. and Dr. Shivashankar, M. (2017). History, method of production, structure and applications of activated carbon. *International Journal of Engineering Research & Technology (IJERT),* 2(3), 23 – 27. ISSN: 2278-0181http:// www.ijert.org

Salehzadeh, J. (2013). Removal of heavy metals Pb^{2+}, Cu^{2+}, Zn^{2+}, Cd^{2+}, Ni^{2+}, Co^{2+} and Fe^{3+} from aqueous solution by using xanthium pensylvanicum. *Leonardo Journal of Sciences,* 1(1)97-104. http://Ijs.academicdirect.org/

Sebata, E., Moyo, M., Guyo, M., Ngano, N. P., Nyamunda, B. C., Chigondo, F., Chitsa, V. and Shumba, M. (2013). Adsorptive removal of atrazine from aqueous solution using bambara groundnut hull (Vigna Subterranean). *International Journal of Engineering Research and Technology*, 2(1), 312 – 321.

Shamsuddin, M. S., Yusoff, N. R. N. and Sulaiman, M. A. (2015). Synthesis and characterization of activated carbon produced from kenaf core fibre using H_3PO_4 activation. *5th International Conference on Recent Advances in Materials and Environment (RAMM) & 2nd International Postgraduate Conference on Material, Mineral and Polymer (MAMIP)*, 19(1), 558-565.

Shigeyuki, B., Hung, T. C., Mio, K., Tomomi, I. and Eric, W. C. C. (2016) Artocarpus tilis and pandanus tectorius: Two important fruit of oceania with medicinal values. *Emirates Journal of Food and Agriculture*, 28(8), 531-539.

Sudha, R. and Premkumar, P. (2016). Lead removal by waste organic plant source materials review. *International Journal of Chem. and Tech Research,* 9(1), 47-57.

Sudha, R., Kalpana, K., Rajachandrasekar, T. and Arivoli, S. (2007). Comparative study on the adsorption kinetics and thermodynamics of metal ion onto acid activated low cost pandanus carbon. *E-Journal of Chemistry*, 4(2), 238 – 254.

Suleiman, I., Jonathan, Y., Ndamitso, M. M. and Crystal, C. A. (2013). Equilibrium and adsorption studies of alachite green onto melon seed shell activated carbon. *International Journal of Modern Chemistry,* 4(2), 90 – 103.

Suleimani, M. and Kaghazchi, T. (2008). Adsorption of gold from industrial wastewater using activated carbon derived from hard shell of apricot stones: An agricultural waste. *International Journal of Bio-resource Technology*, 99(1), 534 - 538.

Taha, N. A., Abdelhafez, S. E. and El-Maghiraby, A. (2016). Chemical and physical preparation of activated carbon using raw bagasse pith for cationic dye adsorption. *Global NEST Journal,* 18(2), 402 – 415.

Zubrik, A., Matik, M., Hredzak, S., Lovas, M., Dankova, Z., Kovacova, M. and Briancin, J. (2017). Preparation of chemically activated carbon from waste biomass by single-stage and two-stage pyrolysis. *Journal of Cleaner Production*, 143(1), 643 - 653.

APPENDIX A

Table A1: Effect of pH on adsorption of Pb^{2+} and Ni^{2+}

pH	Ce (mg/l)		Qe (mg/g)		R(%)	
	Pb	Ni	Pb	Ni	Pb	Ni
2	0.4198	0.1156	7.0067	0.3733	40.0	14.I
4	0.2922	0.1128	10.1976	0.5429	58.3	16.1
6	0.5120	0.1178	4.7027	0.4170	26.9	12.4

8	0.4860	0.1166	5.3528	0.4467	30.6	13.3
10	0.4460	0.1196	6.3523	0.3726	36.3	11.1

Table A.2: Effect of dosage on adsorption of Pb^{2+} and Ni^{2+}

Weight of variation (g)	Ce (mg/l)		Qe (mg/g)		R(%)	
	Pb	Ni	Pb	Ni	Pb	Ni
0.2	0.2329	0.1184	11.6805	0.4013	66.7	12
0.4	0.2164	0.1189	12.0428	0.3902	69.1	11.6
0.6	0.1436	0.1192	13.0127	0.3815	79.5	11.4
0.8	0.1619	0.1192	13.4544	0.3837	76.9	11.4

Table A.3: Effect of contact time on adsorption of Pb^{2+} and Ni^{2+}

Contact time (min)	Ce (mg/l)		Qe (mg/g)		R(%)	
	Pb	Ni	Pb	Ni	Pb	Ni
20	0.3062	0.1143	9.8474	0.5041	56.3	15
40	0.3703	0.1141	8.2441	0.5111	47.1	15.2
60	0.3283	0.1156	9.2961	0.4732	53.1	14.1

80	0.3319	0.1175	9.2058	0.4254	52.6	12.7
100	0.3148	0.1148	9.6318	0.4936	55.6	14.6
120	0.3371	0.1133	9.0757	0.5291	51.6	15.8

Table A.4: Effect of Temperature on adsorption of Pb^{2+} and Ni^{2+}

Temperature	Ce		Qe		R(%)	
(^{o}C)	(mg/l)		(mg/g)			
	Pb	Ni	Pb	Ni	Pb	Ni
30	0.205	0.1221	12.3753	0.3098	70.7	9.2
40	0.2278	0.1208	11.8071	0.3434	67.5	10.2
50	0.2162	0.1216	12.0983	0.322	69.1	9.6
60	0.446	0.1220	11.3871	0.3124	65.1	9.3

APPENDIX B

Table B1: Isotherm Data for Pb^{2+} and Ni^{2+} Adsorption on NaOH-PAC

Metal ion	Ce (mg/l)	Qe (mg/l)	Ce/Qe	LogCe	LogQe	InCe
Pb	0.2051	12.3753	0.0166	-0.6880	1.0926	-1.5843
	0.2278	11.8071	0.0193	-0.6424	1.0721	-1.1479
	0.2162	12.0983	0.0179	-0.6651	1.0827	-1.5316
	0.2446	11.3871	0.0215	-0.6115	1.0564	-1.4081

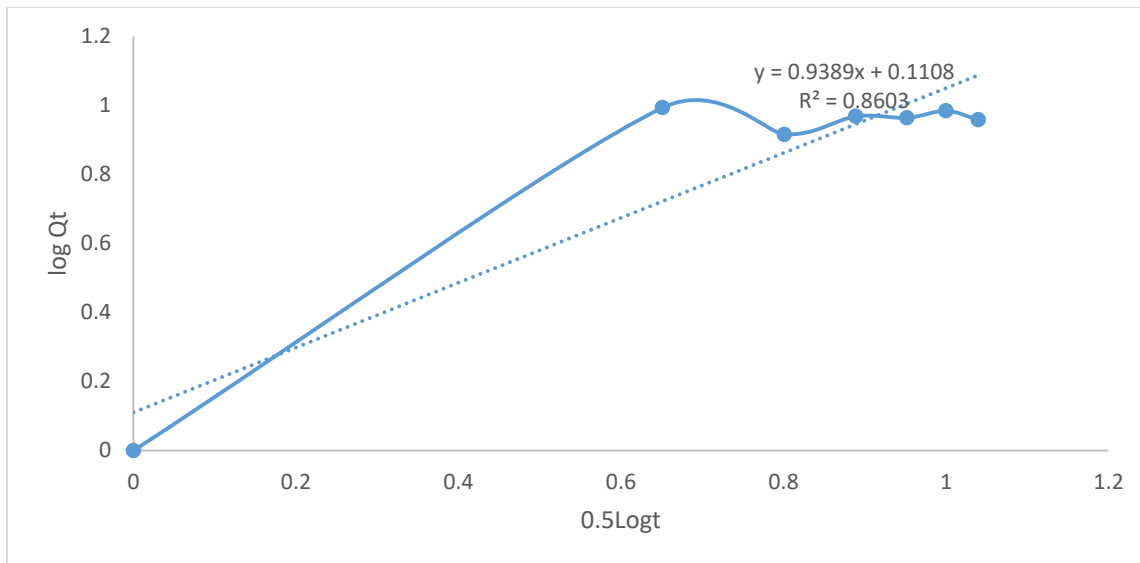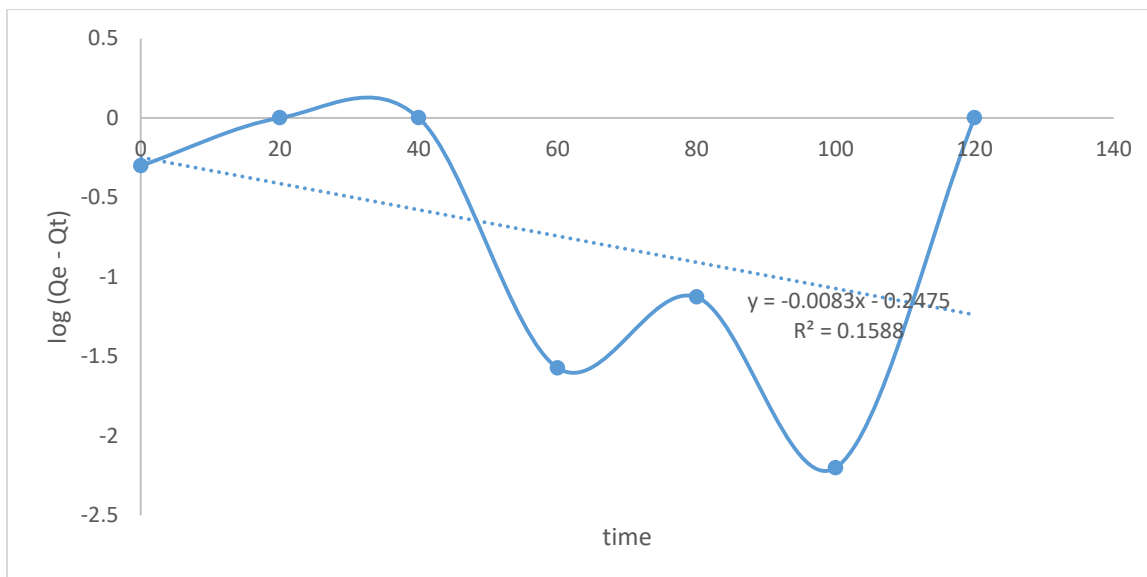| Ni	0.1221	0.3098	0.3941	-0.9133	-0.5089	-2.1029
	0.1208	0.3434	0.3518	-0.9179	-0.4642	-2.1136
	0.1216	0.3220	0.3776	-0.9151	-0.4921	-2.1070
	0.122	0.3124	0.3905	-0.9136	-0.5053	-2.1037

Figure B.1: the first order kinetic studies on Pb^{2+} adsorption on NaOH-PAC
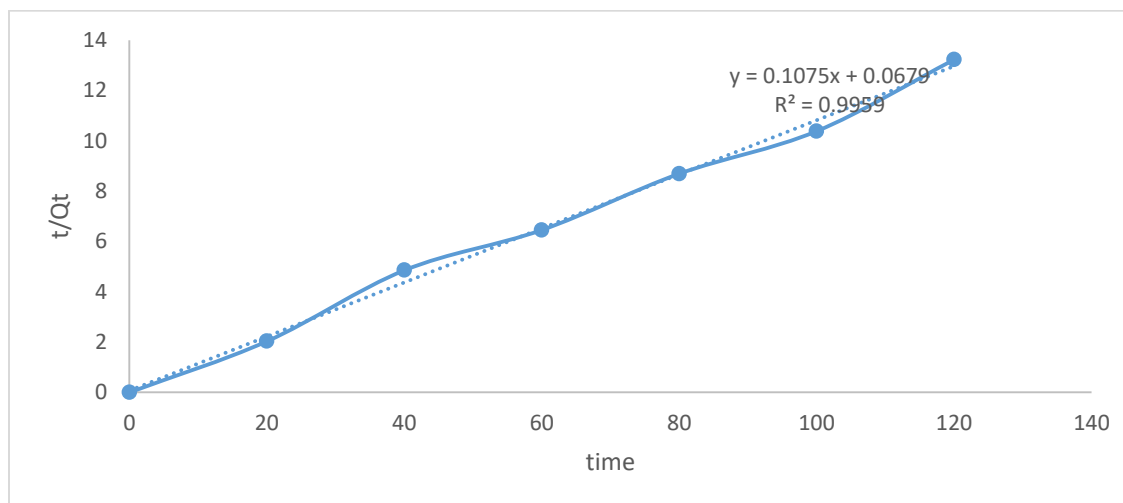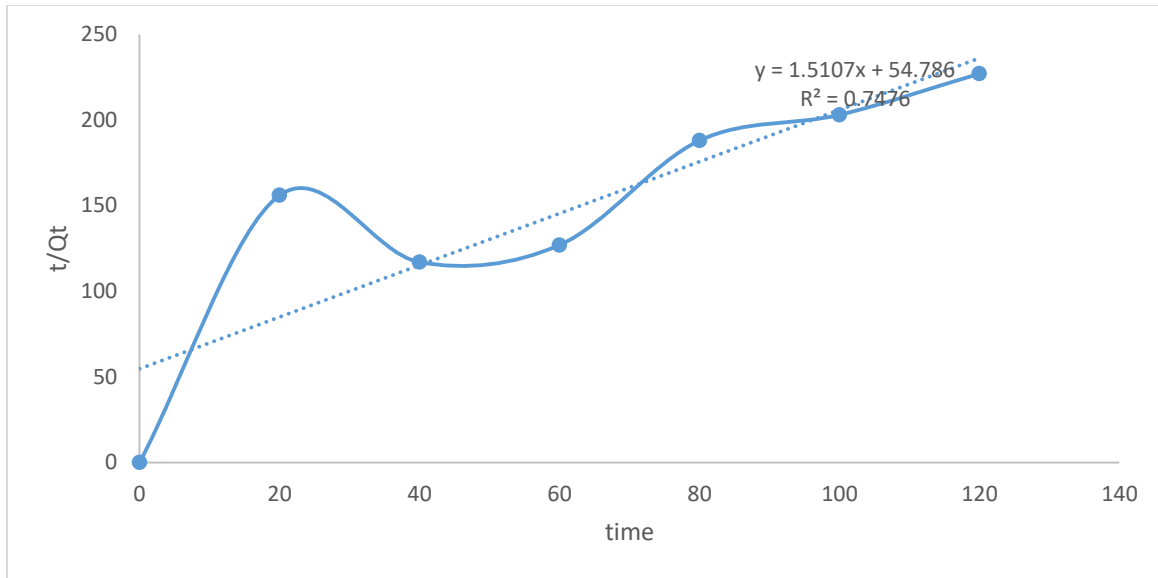

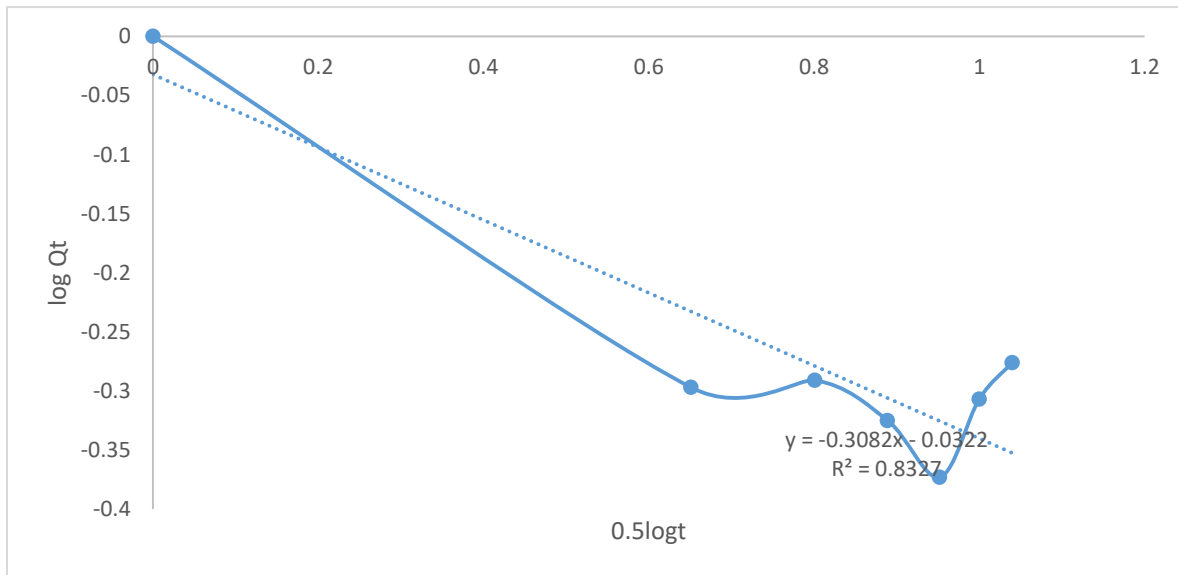**Figure B.2: the second order kinetic studies on Pb^{2+} adsorption on NaOH-PAC**

Figure B.3: The Intra-particle diffusion on Pb^{2+} adsorption on NaOH-PAC

Figure B.4: The first order kinetic studies on Ni^{2+} adsorption on NaOH-PAC

Figure B.5: The second order kinetic studies on Ni^{2+} adsorption on NaOH-PAC

Figure B.6: The intra-particle diffusion on Ni^{2+} adsorption on NaOH-PAC

Table B.7: Isotherm study of Pb^{2+} and Ni^{2+} adsorption on NaOH-PAC

Metal ion	Ce (mg/l)	Qe (mg/l)	Ce/Qe	LogCe	LogQe	InCe
Pb	0.2051	12.3753	0.0166	-0.6880	1.0926	-1.5843

	0.2278	11.8071	0.0193	-0.6424	1.0721	-1.1479
	0.2162	12.0983	0.0179	-0.6651	1.0827	-1.5316
	0.2446	11.3871	0.0215	-0.6115	1.0564	-1.4081
Ni	0.1221	0.3098	0.3941	-0.9133	-0.5089	-2.1029
	0.1208	0.3434	0.3518	-0.9179	-0.4642	-2.1136
	0.1216	0.3220	0.3776	-0.9151	-0.4921	-2.1070
	0.122	0.3124	0.3905	-0.9136	-0.5053	-2.1037